Supplementary material

Manifold neighboring envelope sample projection reconstruction-based imbalanced ensemble algorithm with consistent fuzzy clustering

1. Method

1.1. Notation

Given a training set $\{X,Y\} = \{(x_1,y_1),(x_2,y_2),...,(x_N,y_N)\}$, where y_n expresses the true label of a sample $x_n \in \mathbb{R}^d, n = 1,2,...,N$. The numbers of majority samples and minority samples in the original dataset X are denoted as N_{maj} and N_{min}, respectively. Random resampling of majority class samples is performed to obtain Q subsets, and the number of majority class samples in each subset is N_{min}. The Q subsets of majority class samples are fused with minority class samples to obtain a balanced set of original sample subsets $X_S = \{X^{(1)}, X^{(2)},...,X^{(Q)}\}$, and each subset $X^{(q)}, q = 1,2,...,Q$ includes $N' = 2N_{min}$ samples. Based on each subset $X^{(q)}, q = 1,2,...,Q$, the MNEFD algorithm is implemented to obtain two types of envelope sample subsets: the neighboring envelope sample subset $\tilde{X}^{(q)} \in \mathbb{R}^{N' \times d}$ and the neighboring cluster envelope sample subset $V^{(q)} \in \mathbb{R}^{C \times d}$. Based on the training of $\tilde{X}^{(q)}$ and $V^{(q)}$, $2 \times Q$ base classifiers are obtained, and the predictive label matrix E. The final label $\hat{y}$ is obtained by fusion of the E through a 2D sparse fusion mechanism (2D-SFM).

1.2. Brief description of the proposed method

The main part of the proposed method (MNEFD_IE) is the manifold neighboring envelope learning algorithm (MNEFD) which constructs two types of envelope samples: NES and NCES. Fig. 3 shows the flowchart of the two kinds of imbalanced ensemble algorithms and Table 1 shows the related terminology used in this paper. Fig. 3 (a) shows the framework of the existing imbalanced ensemble algorithms. As shown in Fig. 3 (a), this kind of algorithm is original sample-based methods, since the subsets are derived from the same datasets by resampling. Fig. 3 (b) shows the framework of the proposed method. As shown in Fig. 3 (b), the proposed method is an envelope sample-based method since it generates structured samples for subsequent modeling. Fig. 3 (c) shows the flowchart of the MNEFD algorithm for constructing two types of envelope samples.

The main procedures are outlined as follows: First, this algorithm uses an undersampling method to obtain Q balanced subsets. Second, based on each balanced subset, the local similarity between the samples and their manifold nearest neighbors is mined by the manifold neighboring envelope sample projection reconstruction mechanism (MNESR). Each sample is enveloped with its manifold nearest neighbors to reconstruct it as the neighboring envelope sample. Next, based on the NES, a consistent fuzzy clustering algorithm (CFCMD) is designed to mine the global similarity among samples and map it to the NCES. Then, the MNESR and CFCMD are combined by joint optimization to optimize two types of envelope samples. After that, the base classifiers are separately trained on the two types of

envelope samples subsets. For the Q balanced subsets, the $2 \times Q$ envelope samples subsets are obtained, so the $2 \times Q$ base classifier array is trained. Finally, for each sample, the $2Q$ classification results are obtained and fused by the 2D sparse fusion mechanism (2D-SFM).

(a)

(b)

(c)

Fig. 3. Flow chart of the proposed algorithm: (a) Classical imbalanced ensemble algorithm framework; (b) The proposed algorithm (MNEFD_IE) framework; (c) The MNEFD algorithm flow chart

Table 1. Related terminology used in this paper

Related terminology	Definition
MNESR	Manifold neighboring envelope sample projection reconstruction
CFCMD	Consistent fuzzy clustering
MIDMD	Minimum interlayer discrepancy mechanism based on maximum mean discrepancy
2D-SFM	2D Sparse fusion mechanism
MNEFD	The envelope learning algorithm combining MNESR and CFCMD
MNEFD_IE	The proposed imbalanced ensemble algorithm

1.3. Manifold neighboring envelope learning algorithm (MNEFD)

The MNEFD algorithm combines MNESR and CFCMD to explore the structural information among samples by joint optimization. MNESR aims to mine the local similarity between the sample and its k manifold nearest neighbors, thereby reconstructing this structural information into neighboring envelope samples by enveloping transposition projection. CFCMD aims to explore the global similarity among samples and to map the structural information to clustering centers, thereby generating neighboring cluster envelope samples.

1.3.1. Manifold neighboring envelope sample projection reconstruction (MNESR)

The MNESR conducts sample transformation by enveloping the sample and its k neighbors. Taking $k = 1$ as an example, for sample $\boldsymbol{x}_i \in \mathbb{R}^d$, its nearest neighbor is $\boldsymbol{x}_j$, and their transpositions are $\boldsymbol{x}_i^T$ and $\boldsymbol{x}_j^T$. Then, these two samples are combined to form the neighboring sample matrix (sample enveloping) $\begin{bmatrix} \boldsymbol{x}_i^T & \boldsymbol{x}_j^T \end{bmatrix} \in \mathbb{R}^{d \times 2}$. Assuming a principal component projection based upon this, we can obtain $\begin{bmatrix} \boldsymbol{x}_i^T & \boldsymbol{x}_j^T \end{bmatrix} \cdot \boldsymbol{P} = \begin{bmatrix} \boldsymbol{x}_i^T & \boldsymbol{x}_j^T \end{bmatrix} \cdot \begin{bmatrix} p_{11} & p_{21} \\ p_{12} & p_{22} \end{bmatrix} = \begin{bmatrix} p_{11}\boldsymbol{x}_i^T + p_{12}\boldsymbol{x}_j^T & p_{21}\boldsymbol{x}_i^T + p_{22}\boldsymbol{x}_j^T \end{bmatrix}$. The principal components are concentrated in the first component, because the meaning of the first component is the component that contains the most information among all components. Therefore, taking the first principal component, we can obtain $\tilde{\boldsymbol{x}}_1 = \begin{bmatrix} \boldsymbol{x}_i^T & \boldsymbol{x}_j^T \end{bmatrix} \cdot \begin{bmatrix} p_{11} \\ p_{12} \end{bmatrix}$; then, the new sample is $\tilde{\boldsymbol{x}}_1 = p_{11}\boldsymbol{x}_i^T + p_{12}\boldsymbol{x}_j^T$. Therefore, it can be determined that the intersample correlation can be mined by nearest neighbor enveloping. This not only helps to obtain intersample structural information but also helps to improve sample separability, as discussed above.

For distance measures, Euclidean distance is the most commonly used distance method, but when the dataset does not have a global linear structure, Euclidean distance is not a reasonable data distance measure. The topological manifold structure is generally used to measure high-dimensional nonlinear data, and this data distance metric is called the manifold distance. Based on the manifold distance, we find k nearest neighbors of each sample in the dataset, and then envelop the sample and the neighboring samples into a sample envelope. Based on this sample envelope, a transposition projection is performed to obtain a neighboring envelope sample with structural information. This sample transformation process is called the manifold neighboring envelope sample projection reconstruction mechanism (MNESR).

The principle of MNESR to extract the structural information of similar samples around the original

sample $\boldsymbol{x}_i$ can be viewed as extracting the principal sample of similar samples. This new sample not only contains most of the information of the original sample but also contains the structural information of the similar samples around the original sample $\boldsymbol{x}_i$, which is more helpful for modeling. The mathematical description is as follows.

Consider a subset $\boldsymbol{X}^{(q)}, q = 1, 2, ..., Q$ of $\boldsymbol{X}_S = \left\{ \boldsymbol{X}^{(1)}, \boldsymbol{X}^{(2)}, ..., \boldsymbol{X}^{(Q)} \right\}$ containing N' samples

denoted as the original sample subset $\boldsymbol{X}^{(q)} = \begin{bmatrix} \boldsymbol{x}_1 \\ \boldsymbol{x}_2 \\ \vdots \\ \boldsymbol{x}_{N'} \end{bmatrix} \in \mathbb{R}^{N' \times d}$. Based on the principle of the Isomap

algorithm, the manifold distance between the samples in $\boldsymbol{X}^{(q)}$ is calculated. The neighboring sample envelope is constructed for each sample based on the manifold distance, and the manifold neighboring sample envelope matrix composed of all transposed neighboring sample envelopes is projected to obtain the neighboring envelope sample subset.

Step 1: Computing the neighborhood graph matrix

In the input space X, the Euclidean distance between samples i, j is calculated in turn $d_{\mathrm{X}}(i, j)$ to determine which samples are neighbors on manifold M. Based on $d_{\mathrm{X}}(i, j)$, the k nearest neighbors are taken as neighbors of sample i. These neighborhood relations are represented as a weighted graph G over the samples, with edges of weight $d_{\mathrm{X}}(i, j)$ between neighboring samples.

Step 2: Computing the matrix of shortest paths

The geodesic distances (manifold distances) $d_M(i, j)$ between all sample pairs on the manifold are estimated by computing the shortest path distances $d_G(i, j)$ in graph G. For the neighboring samples, Euclidean distance can better reflect the geodesic distance; the distant samples are approximated by adding the distances between neighboring samples to find the shortest path to the geodesic distance. Therefore, if the sample pairs i, j are linked by an edge, then $d_G(i, j) = d_{\mathrm{X}}(i, j)$; otherwise, let $d_G(i, j) = \infty$, thus obtaining the weighted graph after initialization G. Based on G, $\min \left\{ d_G(i, j), d_G(i, t) + d_G(t, j) \right\}, t = 1, 2, ..., N'$ is calculated in turn to update the shortest path of all sample pairs in $d_G(i, j)$. As the number of samples increases, the graph distances $d_G(i, j)$ can better approximate the manifold distances $d_M(i, j)$.

Step 3: Construction of the manifold neighboring sample envelope

Based on manifold distances $d_M(i, j)$, find the k nearest neighbors of sample $\boldsymbol{x}_i \in \mathbb{R}^d, i = 1, 2, ..., N'$; then envelop them into a manifold neighboring sample envelope

$$\mathcal{M}_i = \begin{bmatrix} \boldsymbol{x}_{i,1} \\ \hat{\boldsymbol{x}}_{i,2} \\ \vdots \\ \hat{\boldsymbol{x}}_{i,j} \\ \vdots \\ \hat{\boldsymbol{x}}_{i,k+1} \end{bmatrix} \in \mathbb{R}^{(k+1)\times d}$$, where the subscript i indicates the sequential number of the original sample

and the subscript j denotes the sequential number of the sample in the sample envelope; after that, the

sample envelope is transposed as $\mathcal{M}_i^T = \begin{bmatrix} \boldsymbol{x}_{i,1}^T & \hat{\boldsymbol{x}}_{i,2}^T & \cdots & \hat{\boldsymbol{x}}_{i,k+1}^T \end{bmatrix} \in \mathbb{R}^{d\times(k+1)}$. Similar processing is

conducted on all the original samples; then, for dataset $\boldsymbol{X}^{(q)}$, N' transposed manifold neighboring

sample envelopes are obtained. These sample envelopes are combined by columns ($\hat{T}$) to obtain a

manifold neighboring sample envelope matrix

$$\boldsymbol{\mathcal{M}}^{\hat{T}} = \begin{bmatrix} \mathcal{M}_1^T \\ \mathcal{M}_2^T \\ \vdots \\ \mathcal{M}_{N'}^T \end{bmatrix} = \begin{bmatrix} \boldsymbol{x}_{1,1}^T & \hat{\boldsymbol{x}}_{1,2}^T & \cdots & \hat{\boldsymbol{x}}_{1,k+1}^T \\ \boldsymbol{x}_{2,1}^T & \hat{\boldsymbol{x}}_{2,2}^T & \cdots & \hat{\boldsymbol{x}}_{2,k+1}^T \\ \vdots & \vdots & \cdots & \vdots \\ \boldsymbol{x}_{N',1}^T & \hat{\boldsymbol{x}}_{N',2}^T & \cdots & \hat{\boldsymbol{x}}_{N',k+1}^T \end{bmatrix} \in \mathbb{R}^{(N'\times d)\times(k+1)}.$$

Step 4: Computing the manifold neighboring envelope sample

Center $\boldsymbol{\mathcal{M}}^{\hat{T}}$, i.e., $\sum_{i=1}^{N'\times d} \boldsymbol{\mathcal{M}}_i^{\hat{T}} = 0$, and then perform sample projection based on the centered $\boldsymbol{\mathcal{M}}^{\hat{T}}$

to obtain $\tilde{\boldsymbol{\mathcal{M}}} = \boldsymbol{\mathcal{M}}^{\hat{T}}\boldsymbol{P} = \begin{bmatrix} \mathcal{M}_1^T\boldsymbol{P} \\ \mathcal{M}_2^T\boldsymbol{P} \\ \vdots \\ \mathcal{M}_{N'}^T\boldsymbol{P} \end{bmatrix} = \begin{bmatrix} \tilde{\mathcal{M}}_1 \\ \tilde{\mathcal{M}}_2 \\ \vdots \\ \tilde{\mathcal{M}}_{N'} \end{bmatrix} \in \mathbb{R}^{(N'\times d)\times 1}$, where $\tilde{\mathcal{M}}_i \in \mathbb{R}^{d\times 1}$ is the neighboring envelope

sample, and $\boldsymbol{P} \in \mathbb{R}^{(k+1)\times 1}$ is the projection vector. Based on the transposition of each envelope sample

$\tilde{\mathcal{M}}_i$, we can obtain the final envelope sample $\tilde{\boldsymbol{x}}_i = \tilde{\mathcal{M}}_i^T = \boldsymbol{P}^T\mathcal{M}_i$. Finally, the original sample subset

$$\boldsymbol{X}^{(q)} = \begin{bmatrix} \boldsymbol{x}_1 \\ \boldsymbol{x}_2 \\ \vdots \\ \boldsymbol{x}_{N'} \end{bmatrix} \in \mathbb{R}^{N'\times d}$$ is transformed to the neighboring envelope sample subset $\tilde{\boldsymbol{X}}^{(q)} = \begin{bmatrix} \tilde{\boldsymbol{x}}_1 \\ \tilde{\boldsymbol{x}}_2 \\ \vdots \\ \tilde{\boldsymbol{x}}_N \end{bmatrix} \in \mathbb{R}^{N'\times d}$.

To obtain the optimal $\boldsymbol{P}$, an objective function is constructed to minimize the reconstruction error
as follows.

$$
\begin{aligned}
J_{MNSER}(\boldsymbol{P}) &= \min_{\boldsymbol{P}} \sum_{i=1}^{N'} \left\| \mathcal{M}_i^T - \tilde{\mathcal{M}}_i\boldsymbol{P}^T \right\|_2^2 \\
&= \min_{\boldsymbol{P}} \sum_{i=1}^{N'} \left\| \mathcal{M}_i^T - \mathcal{M}_i^T\boldsymbol{P}\boldsymbol{P}^T \right\|_2^2 \\
&= \min_{\boldsymbol{P}} \sum_{i=1}^{N'} \left\| \mathcal{M}_i - \boldsymbol{P}\boldsymbol{P}^T\mathcal{M}_i \right\|_2^2 \\
&s.t.\boldsymbol{P}^T\boldsymbol{P} = \boldsymbol{I}
\end{aligned}
\tag{1}
$$

Eq. (1) can be organized as follows.

$$
\begin{aligned}
J_{MNSER}(\boldsymbol{P}) &= \min_{\boldsymbol{P}} \sum_{i=1}^{N'} \left\| \mathcal{M}_i - \boldsymbol{P}\boldsymbol{P}^{\mathrm{T}}\mathcal{M}_i \right\|_2^2 \\
&= \min_{\boldsymbol{P}} \sum_{i=1}^{N'} \mathcal{M}_i^T \mathcal{M}_i - 2\sum_{i=1}^{N'} \mathcal{M}_i^T \boldsymbol{P}\boldsymbol{P}^{\mathrm{T}}\mathcal{M}_i + \sum_{i=1}^{N'} \mathcal{M}_i^T \boldsymbol{P}\boldsymbol{P}^{\mathrm{T}}\boldsymbol{P}\boldsymbol{P}^{\mathrm{T}}\mathcal{M}_i \\
&= \min_{\boldsymbol{P}} \sum_{i=1}^{N'} \mathcal{M}_i^T \mathcal{M}_i - \sum_{i=1}^{N'} \mathcal{M}_i^T \boldsymbol{P}\boldsymbol{P}^{\mathrm{T}}\mathcal{M}_i \\
&= \min_{\boldsymbol{P}} \sum_{i=1}^{N'} \mathcal{M}_i^T \mathcal{M}_i - tr\left[\boldsymbol{P}^{\mathrm{T}}\left(\sum_{i=1}^{N'} \mathcal{M}_i \mathcal{M}_i^T \right) \boldsymbol{P} \right] \\
&= \min_{\boldsymbol{P}} \sum_{i=1}^{N'} \mathcal{M}_i^T \mathcal{M}_i - tr\left[\boldsymbol{P}^{\mathrm{T}}\left(\boldsymbol{\mathcal{M}}^{\hat{T}} \right)^T \boldsymbol{\mathcal{M}}^{\hat{T}} \boldsymbol{P} \right]
\end{aligned}
\tag{2}
$$

In Eq. (2), $\sum_{i=1}^{N'} \mathcal{M}_i^T \mathcal{M}$ is a constant, so Eq. (2) is equivalent to Eq. (3):

$$
\begin{aligned}
J_{MNSER}(\boldsymbol{P}) &= \min_{\boldsymbol{P}} - tr\left(\boldsymbol{P}^{\mathrm{T}}\left(\boldsymbol{\mathcal{M}}^{\hat{T}} \right)^T \boldsymbol{\mathcal{M}}^{\hat{T}} \boldsymbol{P} \right) \\
&s.t.\boldsymbol{P}^{\mathrm{T}}\boldsymbol{P} = \boldsymbol{I}
\end{aligned}
\tag{3}
$$

The objective function $J_{MNSER}(\boldsymbol{P})$ can be optimized by the Lagrange multiplier method to obtain Eq. (4):

$$
J_{MNSER}(\boldsymbol{P}) = -tr\left[\boldsymbol{P}^{\mathrm{T}}\left(\boldsymbol{\mathcal{M}}^{\hat{T}} \right)^T \boldsymbol{\mathcal{M}}^{\hat{T}} \boldsymbol{P} + \zeta\left(\boldsymbol{P}^{\mathrm{T}}\boldsymbol{P} - \boldsymbol{I} \right) \right]
\tag{4}
$$

Solve for the minimalist solution of Eq. (4) to obtain Eq. (5):

$$
\left(\boldsymbol{\mathcal{M}}^{\hat{T}} \right)^T \boldsymbol{\mathcal{M}}^{\hat{T}} \boldsymbol{P} = \zeta \boldsymbol{P}
\tag{5}
$$

From Eq. (5), we can solve that $\boldsymbol{P}$ is a matrix composed of the eigenvectors of $\left(\boldsymbol{\mathcal{M}}^{\hat{T}} \right)^T \boldsymbol{\mathcal{M}}^{\hat{T}}$

and ζ is a diagonal matrix composed of the eigenvalues of $\left(\boldsymbol{\mathcal{M}}^{\hat{T}} \right)^T \boldsymbol{\mathcal{M}}^{\hat{T}}$. Therefore, when we reconstruct the sample envelope consisting of $k+1$ samples into a structured neighboring envelope sample by envelope sample projection reconstruction, we need to find the eigenvector $\boldsymbol{P}$ corresponding to the largest eigenvalue of $\left(\boldsymbol{\mathcal{M}}^{\hat{T}} \right)^T \boldsymbol{\mathcal{M}}^{\hat{T}}$ as the projection vector.

The whole process of the MNESR algorithm is as follows.

Algorithm 1: MNESR
Input: Original sample subset $\boldsymbol{X}^{(q)}$, Number of samples N', Number of manifold nearest neighbors k.
Procedure:
1：Computing the neighborhood graph matrix G;
2：Computing the matrix of shortest paths to approximate the manifold distances $d_M(i,j)$;

3 ： For i-th sample, construct its sample envelope $\mathcal{M}_i = \begin{bmatrix} \boldsymbol{x}_{i,1} \\ \hat{\boldsymbol{x}}_{i,2} \\ \vdots \\ \hat{\boldsymbol{x}}_{i,k+1} \end{bmatrix}$, and the transposed sample envelope

$$\mathcal{M}_i^T = \begin{bmatrix} \boldsymbol{x}_{i,1}^T & \hat{\boldsymbol{x}}_{i,2}^T & \cdots & \hat{\boldsymbol{x}}_{i,k+1}^T \end{bmatrix};$$

4 ： Repeat step 3 until all the samples are processed. After that, the original samples are transformed into the centered

sample envelope matrix $\mathcal{M}^{\hat{T}} = \begin{bmatrix} \mathcal{M}_1^T \\ \mathcal{M}_2^T \\ \vdots \\ \mathcal{M}_{N'}^T \end{bmatrix};$

5 ： For the sample envelope matrix $\mathcal{M}^{\hat{T}}$, the principal samples of every sample envelope are extracted by Eqs. (1)-

(5). Then, the principal samples are the reconstructed envelope samples $\tilde{\boldsymbol{X}}^{(q)} = \begin{bmatrix} \tilde{\boldsymbol{x}}_1 \\ \tilde{\boldsymbol{x}}_2 \\ \vdots \\ \tilde{\boldsymbol{x}}_{N'} \end{bmatrix} \in \mathbb{R}^{N' \times d}$;

6 ： Return $\tilde{\boldsymbol{X}}^{(q)}$;

Output: Neighboring envelope sample subset $\tilde{\boldsymbol{X}}^{(q)}$.

1.3.2. Consistent fuzzy clustering algorithm (CFCMD)

Based on the neighboring envelope sample subset $\tilde{\boldsymbol{X}}^{(q)} = \begin{bmatrix} \tilde{\boldsymbol{x}}_1 \\ \tilde{\boldsymbol{x}}_2 \\ \vdots \\ \tilde{\boldsymbol{x}}_{N'} \end{bmatrix} \in \mathbb{R}^{N' \times d}$, the clustered samples

obtained by fuzzy c-means (FCM) are denoted as $\boldsymbol{V}^{(q)} = \begin{bmatrix} \boldsymbol{v}_1 \\ \boldsymbol{v}_2 \\ \vdots \\ \boldsymbol{v}_C \end{bmatrix} \in \mathbb{R}^{C \times d}$. The objective function of FCM

is expressed as follows:

$$J(\boldsymbol{U}, \boldsymbol{V}^{(q)}) = \min_{\boldsymbol{U}, \boldsymbol{V}^{(q)}} \sum_{i=1}^{N'} \sum_{j=1}^{C} \left(u_{ij} \right)^m \left\| \tilde{\boldsymbol{x}}_i - \boldsymbol{v}_j \right\|^2 \tag{6}$$

$$s.t. \boldsymbol{U}\boldsymbol{1} = \boldsymbol{1}, \quad \boldsymbol{U} \geq 0$$

where $\boldsymbol{U} = \begin{bmatrix} u_{11} & u_{12} & \cdots & u_{1C} \\ u_{21} & u_{22} & \cdots & u_{2C} \\ \cdots & \cdots & \cdots & \cdots \\ u_{N'1} & u_{N'2} & \cdots & u_{N'C} \end{bmatrix} \in \mathbb{R}^{N' \times C}$ is the partition matrix; $\boldsymbol{V}^{(q)}$ is the clustering centers

subset; $\left\| \tilde{\boldsymbol{x}}_i - \boldsymbol{v}_j \right\|_2^2$ denotes the Euclidean distance between sample $\tilde{\boldsymbol{x}}_i \in \tilde{\boldsymbol{X}}^{(q)}$ and cluster center $\boldsymbol{v}_j$;

u_{ij} refers to the membership value, which indicates the degree of sample $\tilde{x}_i$ belongs to cluster center v_j; C is the number of clusters; $m>1$ is the fuzzification coefficient and is usually set to 2; and $\mathbf{1}$ denotes a column vector with all elements being equal to one.

However, in the process of clustering, the distribution differences between the samples before and after clustering are not considered. Therefore, to enhance the representative capability of the clusters for the input samples (neighboring envelope samples) $\tilde{X}^{(q)}$, a mechanism is designed based on maximum mean discrepancy to maintain the consistency of the distribution differences. This mechanism is called the minimum interlayer discrepancy mechanism based on maximum mean discrepancy-MIDMD. The objective function framework can be obtained:

$$
\begin{aligned}
J_{CFCMD}(\boldsymbol{U},\boldsymbol{V}^{(q)}) &= \gamma J_{FCM}(\boldsymbol{U},\boldsymbol{V}^{(q)}) + \mu J_{MIDMD}(\tilde{X}^{(q)},\boldsymbol{V}^{(q)}) \\
&= \min_{\boldsymbol{U},\boldsymbol{V}^{(q)}} \gamma \sum_{i=1}^{N'} \sum_{j=1}^{C} (u_{ij})^m \left\| \tilde{x}_i - v_j \right\|^2 + \mu loss\left(\mathfrak{F}, \tilde{X}^{(q)}, \boldsymbol{V}^{(q)}\right) \\
&\quad s.t. \boldsymbol{U}\mathbf{1}=\mathbf{1}, \quad \boldsymbol{U} \geq 0
\end{aligned}
\tag{7}
$$

where $loss\left(\mathfrak{F}, \tilde{X}^{(q)}, \boldsymbol{V}^{(q)}\right)$ is a measure of the differences in sample distribution between $\tilde{X}^{(q)}$ and $\boldsymbol{V}^{(q)}$, γ and μ are weights of different items, and $\mathfrak{F}$ is the set of functions that are continuous on the topological space $f: \aleph \rightarrow \mathbb{R}$.

$$
loss\left(\mathfrak{F}, \tilde{X}^{(q)}, \boldsymbol{V}^{(q)}\right) = \sup_{f \in \mathfrak{F}} \left(\frac{1}{N'} \sum_{i=1}^{N'} f(\tilde{x}_i) - \frac{1}{C} \sum_{j=1}^{C} f(v_j) \right)
\tag{8}
$$

We propose the unit ball in the reproducing kernel Hilbert space (RKHS) H as the MIDMD function class $\mathfrak{F}$. MIDMD is designed to determine the consistency of the distribution between $\tilde{X}^{(q)}$ and $\boldsymbol{V}^{(q)}$, as in Eq. (9).

$$
J_{MIDMD}\left(\tilde{X}^{(q)}, \boldsymbol{V}^{(q)}\right) = \left\| \frac{1}{N'} \sum_{i=1}^{N'} f(\tilde{x}_i) - \frac{1}{C} \sum_{j=1}^{C} f(v_j) \right\|_{\mathrm{H}}^2
\tag{9}
$$

Using the characteristic kernels to construct the reproducing Hilbert space and to make the distribution between $\tilde{X}^{(q)}$ and $\boldsymbol{V}^{(q)}$ consistent, we optimize $J_{MIDMD}\left(\tilde{X}^{(q)}, \boldsymbol{V}^{(q)}\right)$ with the following objective function.

$$
J_{MIDMD}\left(\tilde{X}^{(q)}, \boldsymbol{V}^{(q)}\right) = \min_{\boldsymbol{U},\boldsymbol{V}^{(q)}} \frac{1}{N'^2} \sum_{i=1}^{N'} \sum_{i'=1}^{N'} \kappa\left(\tilde{x}_i, \tilde{x}_{i'}\right) - \frac{2}{N'C} \sum_{i=1}^{N'} \sum_{j=1}^{C} \kappa\left(\tilde{x}_i, v_j\right) + \frac{1}{C^2} \sum_{j=1}^{C} \sum_{j'=1}^{C} \kappa\left(v_j, v_{j'}\right)
\tag{10}
$$

Thus, the objective function (7) can be written as Eq. (11).

$$
\begin{aligned}
J_{CFCMD}(\boldsymbol{U},\boldsymbol{V}^{(q)}) &= \gamma J_{FCM}(\boldsymbol{U},\boldsymbol{V}^{(q)}) + \mu J_{MIDMD}(\tilde{X}^{(q)},\boldsymbol{V}^{(q)}) \\
&= \min_{\boldsymbol{U},\boldsymbol{V}^{(q)}} \gamma \sum_{i=1}^{N'} \sum_{j=1}^{C} (u_{ij})^m \left\| \tilde{x}_i - v_j \right\|^2 + \mu \left[\frac{1}{N'^2} \sum_{i=1}^{N'} \sum_{i'=1}^{N'} \kappa\left(\tilde{x}_i, \tilde{x}_{i'}\right) - \frac{2}{N'C} \sum_{i=1}^{N'} \sum_{j=1}^{C} \kappa\left(\tilde{x}_i, v_j\right) + \frac{1}{C^2} \sum_{j=1}^{C} \sum_{j'=1}^{C} \kappa\left(v_j, v_{j'}\right) \right] \\
&\quad s.t. \boldsymbol{U}\mathbf{1}=\mathbf{1}, \quad \boldsymbol{U} \geq 0
\end{aligned}
$$

$$
\tag{11}
$$

1.3.3. MNEFD based on joint optimization of MNESR and CFCMD

To better search for the neighboring envelope sample and the neighboring cluster envelope sample, the MNESR and CFCMD are combined by joint optimization. That is, the projection vector, membership value, cluster center, and weights of different items P, U, $V^{(q)}$, η, γ, μ are optimized jointly.

(1) Objective function

The objective function of the proposed algorithm (MNEFD) can be obtained as follows.

$$
\begin{aligned}
J_{MNEFD}\left(P,U,V^{(q)},\eta,\gamma,\mu\right) &= \eta J_{MNSER}\left(P\right)+J_{CFCMD}(U,V^{(q)}) \\
&= \eta J_{MNSER}\left(P\right)+\gamma J_{FCM}(U,V^{(q)})+\mu J_{MIDMD}(\tilde{X}^{(q)},V^{(q)}) \\
&= \min_{P,U,V^{(q)}} \eta\sum_{i=1}^{N'}\left\|\mathcal{M}_i-PP^{\mathrm{T}}\mathcal{M}_i\right\|_2^2+\gamma\sum_{i=1}^{N'}\sum_{j=1}^{C}\left(u_{ij}\right)^m\left\|\tilde{x}_i-v_j\right\|^2 \\
&\quad +\mu\left[\frac{1}{N'^2}\sum_{i=1}^{N'}\sum_{i'=1}^{N'}\kappa\left(\tilde{x}_i,\tilde{x}_{i'}\right)-\frac{2}{N'C}\sum_{i=1}^{N'}\sum_{j=1}^{C}\kappa\left(\tilde{x}_i,v_j\right)+\frac{1}{C^2}\sum_{j=1}^{C}\sum_{j'=1}^{C}\kappa\left(v_j,v_{j'}\right)\right]
\end{aligned}
\tag{12}
$$

Since $\tilde{x}_i = P^{\mathrm{T}}\mathcal{M}_i$, then the objective function can be transformed into Eq. (13):

$$
\begin{aligned}
J_{MNEFD}\left(P,U,V^{(q)},\eta,\gamma,\mu\right) &= \eta J_{MNSER}\left(P\right)+J_{CFCMD}(P,U,V^{(q)}) \\
&= \eta J_{MNSER}\left(P\right)+\gamma J_{FCM}(P,U,V^{(q)})+\mu J_{MIDMD}(P,V^{(q)}) \\
&= \min_{P,U,V^{(q)}} \eta\sum_{i=1}^{N'}\left\|\mathcal{M}_i-PP^{\mathrm{T}}\mathcal{M}_i\right\|_2^2+\gamma\sum_{i=1}^{N'}\sum_{j=1}^{C}\left(u_{ij}\right)^m\left\|P^{\mathrm{T}}\mathcal{M}_i-v_j\right\|_2^2 \\
&\quad +\mu\left[\frac{1}{N'^2}\sum_{i=1}^{N'}\sum_{i'=1}^{N'}\kappa\left(P^{\mathrm{T}}\mathcal{M}_i,P^{\mathrm{T}}\mathcal{M}_{i'}\right)-\frac{2}{N'C}\sum_{i=1}^{N'}\sum_{j=1}^{C}\kappa\left(P^{\mathrm{T}}\mathcal{M}_i,v_j\right)+\frac{1}{C^2}\sum_{j=1}^{C}\sum_{j'=1}^{C}\kappa\left(v_j,v_{j'}\right)\right] \\
& s.t.\ U1=1,\ \ U\geq0,\ \ P^{\mathrm{T}}P=I
\end{aligned}
\tag{13}
$$

Among them, η,γ,μ are three hyperparameters, and this paper optimizes the hyperparameters based on the grid search method. The right end of Eq. (13) consists of three parts. The first part describes the loss of the manifold neighboring envelope sample reconstruction consisting of $\mathcal{M}_i$ and P. The second part describes the clustering loss measure consisting of $V^{(q)}$ and U. The third part describes the distribution differences between $\tilde{X}^{(q)}$ and $V^{(q)}$.

(2) Optimization

In the MNEFD model, there are three variables P, U and $V^{(q)}$ that need to be optimized. An effective alternating variable optimization strategy can be considered, i.e., to solve for one variable while fixing the rest of the variables as constants. Therefore, in solving objective function (13), P, U and $V^{(q)}$ can be solved in turn using the gradient descent method, and the optimization is described as follows.

1) Fixing $V^{(q)}$ and U to solve P.

By fixing $V^{(q)}$ and U, the problem is solved with respect to P. After removing the terms unrelated to P, the objective function (13) is transformed into Eq. (14).

$$
\begin{aligned}
J_1\left(P,U,V^{(q)}\right) &= \min_{P} \eta\sum_{i=1}^{N'}\left\|\mathcal{M}_i-PP^{\mathrm{T}}\mathcal{M}_i\right\|_2^2+\gamma\sum_{i=1}^{N'}\sum_{j=1}^{C}\left(u_{ij}\right)^m\left\|P^{\mathrm{T}}\mathcal{M}_i-v_j\right\|_2^2 \\
&\quad +\mu\left[\frac{1}{N'^2}\sum_{i=1}^{N'}\sum_{i'=1}^{N'}\kappa\left(P^{\mathrm{T}}\mathcal{M}_i,P^{\mathrm{T}}\mathcal{M}_{i'}\right)-\frac{2}{N'C}\sum_{i=1}^{N'}\sum_{j=1}^{C}\kappa\left(P^{\mathrm{T}}\mathcal{M}_i,v_j\right)\right]+\lambda\left(P^{\mathrm{T}}P-I\right)
\end{aligned}
\tag{14}
$$

As shown in Eq. (14), it is difficult to obtain the closed-form solution of P. Therefore, the gradient descent method is used to update P. Then the iterative solution of P can be expressed as Eq. (15).

$$P_{K+1} = P_K - \theta \cdot \nabla(P) \tag{15}$$

$$
\begin{aligned}
\nabla(P) = &-2\eta \sum_{i=1}^{N'} \left[\left(\mathcal{M}_i - PP^{\mathrm{T}} \mathcal{M}_i \right) \mathcal{M}_i^{\mathrm{T}} P + \mathcal{M}_i \left(\mathcal{M}_i - PP^{\mathrm{T}} \mathcal{M}_i \right)^{\mathrm{T}} P \right] \\
&+2 \sum_{i=1}^{N'} \sum_{j=1}^{C} \left[\gamma \left(u_{ij} \right)^m + \frac{\mu}{N'C\sigma^2} \kappa \left(P^{\mathrm{T}} \mathcal{M}_i, v_j \right) \right] \mathcal{M}_i \left(P^{\mathrm{T}} \mathcal{M}_i - v_j \right)^{\mathrm{T}} \\
&-\frac{\mu}{N'^2\sigma^2} \sum_{i=1}^{N'} \sum_{i'=1}^{N'} \kappa \left(P^{\mathrm{T}} \mathcal{M}_i, P^{\mathrm{T}} \mathcal{M}_{i'} \right) \left(\mathcal{M}_i - \mathcal{M}_{i'} \right) \left(\mathcal{M}_i - \mathcal{M}_{i'} \right)^{\mathrm{T}} P + 2\lambda P
\end{aligned} \tag{16}
$$

2) Fixing P and $V^{(q)}$ to solve U.

By fixing P and $V^{(q)}$, the problem is solved with respect to U. After removing the terms unrelated to U, the objective function (13) is transformed into Eq. (17).

$$J_2(P,U,V^{(q)}) = \min_{U} \gamma \sum_{i=1}^{N'} \sum_{j=1}^{C} \left(u_{ij} \right)^m \left\| P^{\mathrm{T}} \mathcal{M}_i - v_j \right\|_2^2 + \rho \left(\sum_{j=1}^{C} u_{ij} - 1 \right) \tag{17}$$

To the minimal value of Eq. (17), we set.

$$\frac{\partial J_2(P,U,V^{(q)})}{\partial u_{ij}} = m\gamma \left(u_{ij} \right)^{m-1} \left\| P^{\mathrm{T}} \mathcal{M}_i - v_j \right\|_2^2 + \rho = 0 \tag{18}$$

By calculation, the iterative formula of the affiliation matrix is obtained as follows.

$$u_{ij} = \frac{\left(1 / \left\| P^{\mathrm{T}} \mathcal{M}_i - v_j \right\|_2^2 \right)^{\frac{1}{m-1}}}{\sum_{w=1}^{C} \left(1 / \left\| P^{\mathrm{T}} \mathcal{M}_i - v_w \right\|_2^2 \right)^{\frac{1}{m-1}}} \tag{19}$$

3) Fixing U and P to solve $V^{(q)}$.

By fixing U and P, the problem is solved with respect to $V^{(q)}$. After removing the terms unrelated to $V^{(q)}$, the objective function (13) is transformed into Eq. (20).

$$J_3(P,U,V^{(q)}) = \min_{V^{(q)}} \gamma \sum_{i=1}^{C} \sum_{j=1}^{N'} \left(u_{ij} \right)^m \left\| P^{\mathrm{T}} \mathcal{M}_i - v_j \right\|_2^2 + \mu \left[\frac{1}{C^2} \sum_{j=1}^{C} \sum_{j'=1}^{C} \kappa \left(v_j, v_{j'} \right) - \frac{2}{N'C} \sum_{i=1}^{N'} \sum_{j=1}^{C} \kappa \left(P^{\mathrm{T}} \mathcal{M}_i, v_j \right) \right]$$

$$\tag{20}$$

Based on the characteristic Gaussian kernel function $\kappa(x,y) = \exp\left(-\left\| x - y \right\|^2 / 2\sigma^2 \right)$, the objective function (20) is transformed into Eq. (21).

$$\frac{\partial J_3(P,U,V^{(q)})}{\partial v_j} = -2 \sum_{i=1}^{N'} \left[\gamma \left(u_{ij} \right)^m + \frac{\mu}{N'C\sigma^2} \kappa \left(P^{\mathrm{T}} \mathcal{M}_i, v_j \right) \right] \left(P^{\mathrm{T}} \mathcal{M}_i - v_j \right) + \frac{2\mu}{C^2\sigma^2} \sum_{j'=1}^{C} \left(v_{j'} - v_j \right) \kappa \left(v_{j'}, v_j \right)$$

$$\tag{21}$$

Solve for the minimum solution of Eq. (21). $V^{(q)}$ is obtained from Eq. (22).

$$V^{(q)} = A^{-1} \begin{bmatrix} b_1 \\ b_2 \\ \vdots \\ b_C \end{bmatrix} \tag{22}$$

Among them:

$$A = diag(a_1, a_2, ..., a_C) + \frac{\mu}{C^2 \sigma^2} \hat{K}$$

$$\hat{K} = \begin{bmatrix} \kappa(v_1, v_1) & \kappa(v_2, v_1) & ... & \kappa(v_C, v_1) \\ \kappa(v_1, v_2) & \kappa(v_2, v_2) & ... & \kappa(v_C, v_2) \\ ... & ... & ... & ... \\ \kappa(v_1, v_C) & \kappa(v_2, v_C) & ... & \kappa(v_C, v_C) \end{bmatrix}$$

$$a_w = \sum_{i=1}^{N'} \left[\gamma(u_{iw})^m + \frac{\mu}{N'C\sigma^2} \kappa\left(P^T \mathcal{M}_i, v_w \right) \right] - \frac{\mu}{C^2 \sigma^2} \sum_{j=1}^{C} \kappa\left(v_j, v_w \right), w = 1, 2, ..., C$$

$$b_j = \sum_{i=1}^{N'} \left[\gamma\left(u_{ij} \right)^m + \frac{\mu}{N'C\sigma^2} \kappa\left(P^T \mathcal{M}_i, v_j \right) \right] P^T \mathcal{M}_i, \quad j = 1, 2, ..., C$$

The overall process of the MNEFD algorithm is outlined as follows.

Algorithm 2: MNEFD

Input: Original sample subset $X^{(q)}$, Number of manifold nearest neighbors k, Number of clusters C, Iteration number t, Iteration threshold ε.

Procedure:

1：Based on the original sample subset $X^{(q)}$, obtain the initialized neighboring envelope sample subset $\tilde{X}^{(q)}$ and the initialized projection vector P by Algorithm 1 (MNESR);

2：Initialize $V^{(q)}$ and U based on $\tilde{X}^{(q)}$ by FCM algorithm;

3：Optimize the P, U, $V^{(q)}$ by Eqs. (15), (19), and (22), respectively until $\left| J_{MNEFD}^{(t+1)} - J_{MNEFD}^{(t)} \right| < \varepsilon$;

4：Return final P, U, $V^{(q)}$;

5：Based on P, obtain optimized $\tilde{X}^{(q)}$;

Output: Neighboring envelope sample subset $\tilde{X}^{(q)}$, Neighboring cluster envelope sample subset $V^{(q)}$.

1.4. 2D Sparse fusion mechanism (2D-SFM)

According to the obtained envelope samples, the Q subsets of original samples are transformed to $2 \times Q$ subsets of envelope samples, generating $2 \times Q$ prediction results. Because these prediction results (prediction labels) are homogeneous, they can be transformed into a fusion of $1 \times 2Q$ prediction labels. Therefore, the fusion of the $2 \times Q$ prediction results is transformed into a fusion of $1 \times 2Q$ prediction results. The matrix composed of the prediction labels is denoted as

$$E = \begin{bmatrix} e_1 \\ e_2 \\ \vdots \\ e_{N_t} \end{bmatrix} = \begin{bmatrix} e_{11} & e_{12} & ... & e_{1(2Q)} \\ e_{21} & e_{22} & ... & e_{2(2Q)} \\ \vdots & \vdots & ... & \vdots \\ e_{N_t 1} & e_{N_t 2} & ... & e_{N_t(2Q)} \end{bmatrix} \in \mathbb{R}^{N_t \times 2Q}$$, and N_t is the number of test samples in the test set. The

objective function of this sparse fusion mechanism is:

$$\min_{\beta} \left(\| y \text{-} E\beta \|_2^2 + \omega \|\beta\|_1 \right) = \min_{\beta} \left[\sum_{i=1}^{N_t} \left(y_i - \sum_{j=1}^{2Q} e_{ij} \beta_j \right)^2 + \omega \sum_{j=1}^{2Q} |\beta_j| \right] \tag{23}$$

In Eq. (23), $\mathbf{y} = \begin{bmatrix} y_1 \\ y_2 \\ \vdots \\ y_{N_t} \end{bmatrix} \in \mathbb{R}^{N_t \times 1}$ is the true label, $\boldsymbol{\beta} = \begin{bmatrix} \beta_1 \\ \beta_2 \\ \vdots \\ \beta_{2Q} \end{bmatrix} \in \mathbb{R}^{2Q \times 1}$ is the weight vector, and ω

is the penalty coefficient for parameter estimation. The weight of each classifier is calculated by

minimizing the objective function, and the estimated weight vector is $\boldsymbol{\beta}' = \begin{bmatrix} \beta_1' \\ \beta_2' \\ \vdots \\ \beta_{2Q}' \end{bmatrix} \in \mathbb{R}^{2Q \times 1}$. Based on this

weight vector, the final predicted labels are obtained by weighting and summing the labels as

$$\hat{\mathbf{y}} = \Phi\left(\mathbf{E}\boldsymbol{\beta}'\right) \in \mathbb{R}^{N_t \times 1} \tag{24}$$

where, $\Phi(a) = \begin{cases} 0, a \le 0.5 \\ 1, a > 0.5 \end{cases}$.

The imbalanced ensemble algorithm of this paper (MNEFD_IE) is proposed based on MNEFD and 2D-SFM. The pseudocode of MNEFD_IE is provided in Algorithm 3.

Algorithm 3: MNEFD_IE

Input: Original training set $\mathbf{X}$, Number of minority class samples in original training set N_{min}, Number of sample subsets Q, Number of manifold nearest neighbors k, Iteration number t, Iteration threshold ε.

Procedure:

1：Based on the majority class samples in $\mathbf{X}$, we obtain Q majority class sample subsets with the number of samples N_{min} by random undersampling. In addition, the Q majority class sample subsets are fused with minority class samples, respectively, to obtain Q balanced original sample subsets $\mathbf{X}_S = \left\{ \mathbf{X}^{(1)}, \mathbf{X}^{(2)}, ..., \mathbf{X}^{(Q)} \right\}$;

2：For $q = 1 : Q$

3：   Based on the original sample subset $\mathbf{X}^{(q)}$, obtain neighboring envelope sample subset $\tilde{\mathbf{X}}^{(q)}$ and neighboring cluster envelope sample subset $\mathbf{V}^{(q)}$ by MNEFD algorithm;

4：   The classifier $C_1^{(q)}$ is trained based on $\tilde{\mathbf{X}}^{(q)}$;

5：   The classifier $C_2^{(q)}$ is trained based on $\mathbf{V}^{(q)}$;

6：End

7：The prediction label matrix $\mathbf{E}$ is obtained by predicting the test set based on the $2Q$ classifiers;

8：The 2D sparse fusion mechanism (2D SFM) is used to obtain the final labels $\hat{\mathbf{y}}$;

9：Accuracy, AUC, F-measure and G-mean are obtained.

Output: Accuracy, AUC, F-measure, G-mean.

2.　Experimental studies

To demonstrate the performance of the proposed algorithm (MNEFD_IE), groups of experiments were conducted and analyzed. First, the experimental environment is introduced. Second, the effects of relevant parameters on the performance of the proposed algorithm are analyzed. Third, ablation

experiments are conducted for verification of the proposed algorithm. Finally, the proposed algorithm is compared with some representative classical and state-of-the-art imbalanced ensemble algorithms.

2.1. Experimental conditions

Since most of the imbalanced ensemble algorithms choose decision trees as base classifiers, decision tree C 4.5 is chosen as the base classifier here. The 5-fold cross-validation (5-CV) method is chosen. To avoid randomness, each experiment is repeated 5 times and the mean and standard deviation of the values are reported.

2.1.1. Datasets

The 38 representative public datasets are chosen from the KEEL and UCI databases, which are chosen from different domains, with different dimensions, numbers of samples, and imbalance ratios (1.82-100.14). Table 2 provides the basic information of these datasets.

Table 2. Basic information of imbalanced datasets

ID	Name	Features	Samples	Minority	Majority	Imbalance ratio
1	Glass1	9	214	76	138	1.82
2	Wisconsin	9	683	239	444	1.86
3	Pima	8	768	268	500	1.87
4	Iris0	4	150	50	100	2.00
5	Yeast1	8	1484	429	1055	2.46
6	Haberman	3	306	81	225	2.78
7	Vehicle2	18	846	218	628	2.88
8	Vehicle3	18	846	212	634	2.99
9	Glass-0-1-2-3-vs-4-5-6	9	214	51	163	3.20
10	Vehicle0	18	846	199	647	3.25
11	Ecoli1	7	336	77	259	3.36
12	Ecoli2	7	336	52	284	5.46
13	Glass6	9	214	29	185	6.38
14	Yeast3	8	1484	163	1321	8.10
15	Ecoli3	7	336	35	306	8.60
16	Yeast-2-vs-4	8	514	51	463	9.08
17	Yeast-0-5-6-7-9-vs-4	8	528	51	477	9.35
18	Glass-0-1-6-vs-2	9	192	17	175	10.29
19	Glass2	9	214	17	197	11.59
20	Yeast-1-vs-7	8	459	30	429	14.30
21	Glass4	9	214	13	201	15.47
22	Ecoli4	7	336	20	316	15.80
23	Abalone9-18	8	731	42	689	16.40
24	Shuttle-c2-vs-c4	9	129	6	123	20.50
25	Glass5	9	214	9	205	22.78
26	Yeast-2-vs-8	8	482	20	462	23.10
27	Yeast4	8	1484	51	1433	28.10
28	Winequality-red-4	11	1599	53	1506	29.17
29	Yeast-1-2-8-9-vs-7	8	947	30	917	30.57

30	Yeast5	8	1484	44	1440	32.73
31	Yeast6	8	1484	35	1449	41.40
32	Winequality-white-3-vs-7	11	900	20	880	44.00
33	Winequality-red-8-vs-6-7	11	855	18	837	46.50
34	Kr-vs-k-zero-vs-eight	6	1460	27	1433	53.07
35	Shuttle-2-vs-5	9	3316	49	3267	66.67
36	Kddcup-buffer-overflow-vs-back	41	2233	30	2203	73.43
37	Kr-vs-k-zer-v-fifteen	6	2193	27	2166	80.22
38	Rootkit-imapvsback	41	2225	22	2203	100.14

2.1.2. Parameter setting

The important parameters of the proposed algorithm are as follows: (1) Number of sample subsets: Q. (2) Number of manifold nearest neighbors in MNESR: $MN-num$. (3) Number of clustering centers (proportion of clustering centers to the samples before clustering) in CFCMD: $C-num$. For most experiments, these three parameters are set as: $Q=10$, $MN-num=1$, $C-num=50\%$. Three hyperparameters η, γ, μ are involved, which determine the contribution of different loss items in the objective function. The range of the hyperparameters is set to $\eta, \gamma, \mu = \left[10^{-5}, 10^{-4}, ..., 10^{2}\right]$, based on which the grid search method is used to obtain the optimum value. As different value sets (η, γ, μ) are combined, the corresponding best results are selected for each dataset when executing MNEFD_IE. The parameter settings of the classical imbalanced ensemble algorithms are: Number of subsets=10. Other parameters are default.

2.1.3. Evaluation metrics and non-parametric statistical tests

In this paper, we evaluate the performance of each method based on Accuracy (ACC), AUC, F-measure (F-M), and G-mean (G-M) criteria. These evaluation metrics are calculated as follows.

$$Accuracy(ACC) = \frac{TP + TN}{TP + FP + TN + FN}$$

$$AUC = \frac{Sensitivity + Specificity}{2}$$

$$F - measure = \frac{2 * Recall * Precision}{Recall + Precision}$$

$$G - mean = \sqrt{\frac{TP}{TP + FN} * \frac{TN}{TN + FP}}$$

Where TP denotes true positive, FP denotes false positive, TN denotes true negative and FN denotes false negative. In addition, sensitivity, specificity, recall, and precision are calculated as follows.

$$Sensitivity = \frac{TP}{TP + FN}$$

$$Specificity = \frac{TN}{TN + FP}$$

$$Recall = \frac{TP}{TP + FN}$$

$$Precision = \frac{TP}{TP + FP}$$

To determine whether there is a significant difference between the algorithms, we use two kinds of nonparametric statistical tests. (1) Multiple comparisons, based on the Friedman test with its corresponding post hoc test to determine whether there are significant differences between all comparison algorithms. In this paper, the Holm post hoc test was chosen, and the significance level was set at $\alpha = 0.05$. (2) Pairwise comparisons, wherein the Wilcoxon paired signed-rank test was used to determine whether there was a significant difference in the classification ability between the two algorithms. This was complemented by the ranking of all compared algorithms with respect to different evaluation metrics based on the Friedman aligned rank test, where a lower rank number indicates better classification ability.

2.2. Parameter analysis

In this section, the influences of two important parameters: the number of manifold nearest neighbors $MN\text{-}num$ and the number of clustering centers $C\text{-}num$ on the performance of MNEFD_IE is studied. In addition, the optimization of three hyperparameters η, γ, μ is analyzed based on the grid search method.

2.2.1. Effect analysis of the number of manifold nearest neighbors

$MN\text{-}num$ is the number of manifold nearest neighbors selected based on each sample when performing the MNESR. In the proposed algorithm, $MN\text{-}num$ means the number of samples in each sample envelope. This will affect the structural information in the neighboring envelope samples, which in turn affects the classification performance and diversity of the base classifier trained on the subsets indirectly. To investigate the effect of $MN\text{-}num$ on the performance of MNEFD_IE, six datasets with different imbalance ratios (1.86-28.10) are selected for parametric analysis at $MN\text{-}num = 0, 1, 2, 3, 4, 5$. Fig. 4 shows the four evaluation metrics based on different $MN\text{-}num$ for different datasets.
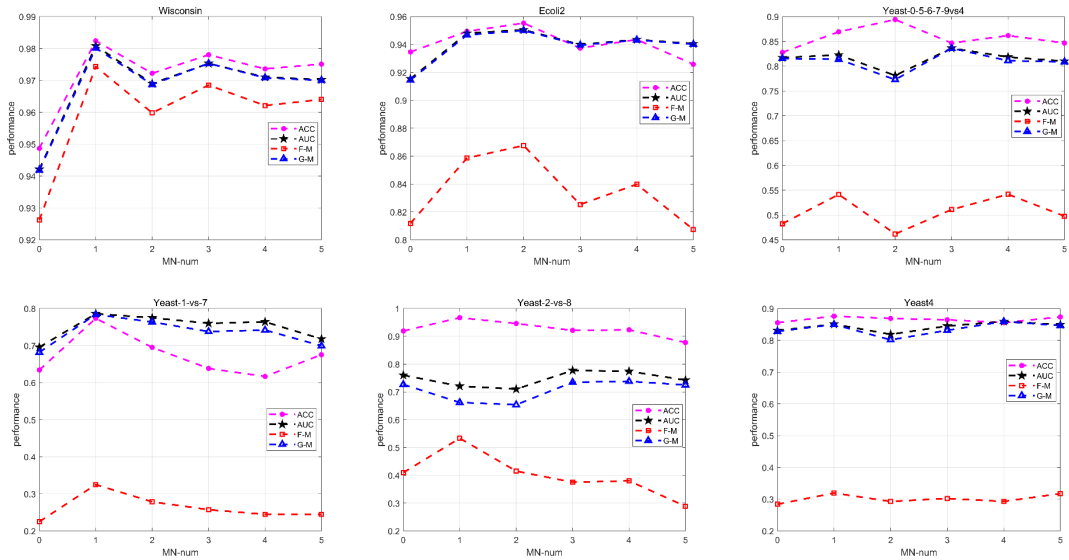

Fig. 4. MNEFD_IE performance with different $MN\text{-}num$

As shown in Fig. 4, when $MN\text{-}num$ changes from 0 to 1, each evaluation metric generally improves to a certain extent, which shows that the introduction of a neighboring sample is effective. The

possible reason for this is that the envelope sample projection reconstruction can effectively explore the local similarity between samples, thus improving the stability and generalization of samples. However, as $MN\text{-}num$ increases, the performance no changes or starts to decrease. Therefore, an excessive value of $MN\text{-}num$ is not suitable, probably because too many selected nearest neighbors increase the redundant information. Therefore, a reasonable value of $MN\text{-}num$ ranges from 1 to 3. To balance the accuracy and computational complexity, this paper sets $MN\text{-}num=1$.

2.2.2. Effect analysis of the number of clusters

$C\text{-}num$ is the ratio of the number of clusters to the number of samples before clustering when performing clustering. The smaller $C\text{-}num$ is, the more compact the mined structural information will be, yet the larger the risk of missing useful structural information. The reverse is also true.

To investigate the effect of $C\text{-}num$ on the performance of MNEFD_IE, six datasets with different imbalance ratios (1.86-28.10) were selected at $C\text{-}num=30\%,40\%,50\%,60\%,70\%,80\%$. Fig. 5 shows the four evaluation metrics in terms of different $C\text{-}num$ and datasets.
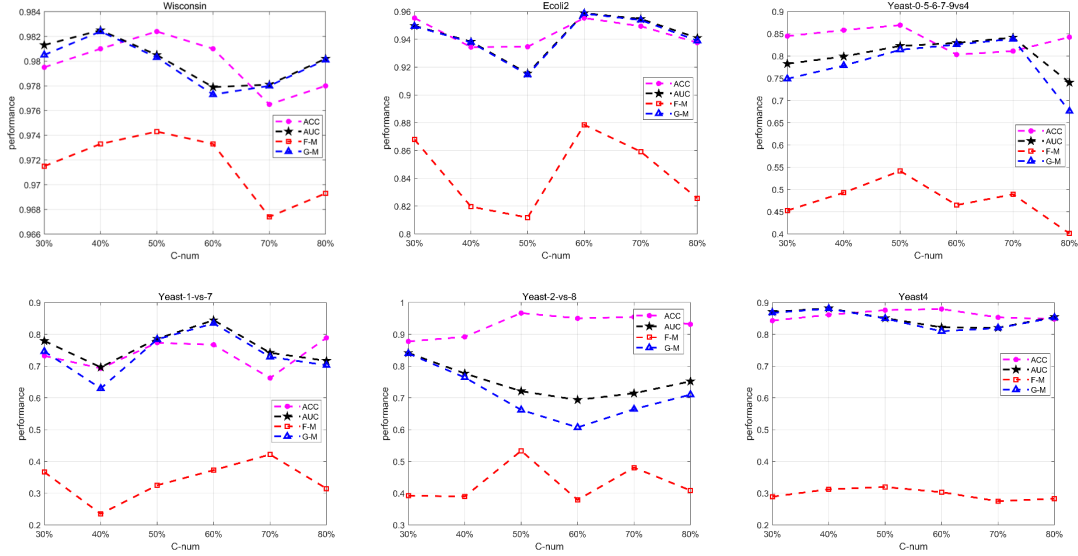
Fig. 5. MNEFD_IE performance with different $C\text{-}num$

As shown in Fig. 5, with the growth of $C\text{-}num$, the performance of the algorithm based on each evaluation metric tends to increase and then decrease, and the best performance is generally obtained when the $C\text{-}num$ is approximately 50%. The $C\text{-}num$ should not be too large or too small: if it is too large, some poor-quality neighboring envelope samples will be generated, and if it is too small, useful information may be lost. Therefore, a reasonable value of $C\text{-}num$ should be chosen from 40% to 60%. To balance the accuracy and computational complexity, this paper sets $C\text{-}num=50\%$.

2.2.3. Effect analysis of hyperparameters

The objective function of the proposed algorithm involves three hyperparameters η, γ and μ, and these three hyperparameters determine the contribution of the different loss items.
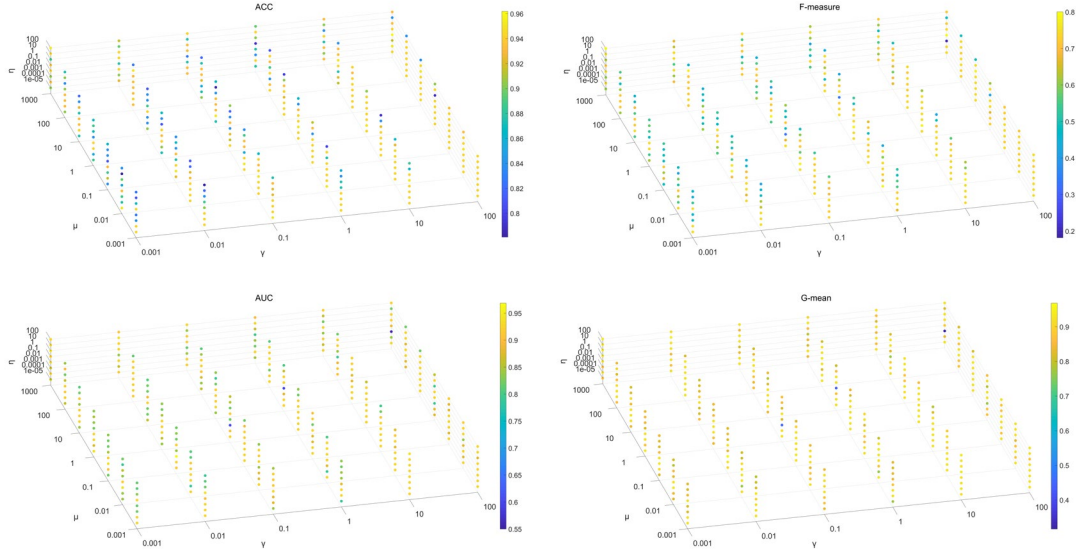
Fig. 6. MNEFD_IE performance with different (η, γ, μ)

To analyze the impacts of these hyperparameters, the performance of MNEFD_IE with different parameter value sets executed on Yeast-0-6-5-7-9-vs-4 is shown in Fig. 6. The color of each point in Fig. 6 denotes the ACC, F-M, AUC, and G-M values for the corresponding parameter values (η, γ, μ). It can be found in Fig. 6 that better performance can be produced with relatively large values of γ and μ and a moderate value of η. The values of γ and μ of approximately 10 and the value of η of approximately 1 could be potential suitable ones.

2.3. Ablation study

To verify the effectiveness of the proposed algorithm, ablation experiment was conducted on six datasets with different imbalance ratios (1.86-28.10). The proposed algorithm is compared with the 'Random_based' and 'MNESR_based' algorithms. 'Random_based' means that the balanced subsets are divided based on random undersampling, as performed by most of the existing ensemble learning algorithms. 'MNESR_based' algorithm means that the subsets balanced by random resampling are handled by MNESR. The comparison of the above three algorithms is presented in Table 3.

Table 3. Ablation results for the proposed method

Dataset	Algorithms	ACC(%)	AUC(%)	F-M(%)	G-M(%)
Wisconsin	'Random_based'	0.9400±0.0400	0.9403±0.0377	0.9178±0.0524	0.9400±0.0377
	'MNESR_based'	0.9765±0.0168	0.9770±0.0212	0.9666±0.0249	0.9769±0.0214
	MNEFD_IE	**0.9898±0.0083**	**0.9921±0.0064**	**0.9857±0.0115**	**0.9921±0.0065**
Ecoli2	'Random_based'	0.9314±0.0482	0.9118±0.0620	0.8079±0.1261	0.9095±0.0655
	'MNESR_based'	0.9349±0.0367	0.9311±0.0512	0.8192±0.0927	0.9307±0.0514
	MNEFD_IE	**0.9761±0.0257**	**0.9538±0.0291**	**0.9242±0.0787**	**0.9532±0.0293**
Yeast-0-5-6-7-9-vs-4	'Random_based'	0.7899±0.0483	0.8497±0.0627	0.4642±0.0765	0.8453±0.0607
	'MNESR_based'	0.7916±0.0803	0.8596±0.0622	0.4811±0.1021	0.8537±0.0647
	MNEFD_IE	**0.9263±0.0039**	**0.9235±0.0779**	**0.6977±0.0370**	**0.9184±0.0873**
Yeast-1-vs-7	'Random_based'	0.7321±0.0963	0.8102±0.0401	0.3179±0.0587	0.7973±0.0409
	'MNESR_based'	0.7868±0.1449	0.7930±0.0604	0.3716±0.1134	0.7784±0.0749
	MNEFD_IE	**0.8110±0.0531**	**0.8214±0.0294**	**0.3732±0.0614**	**0.8210±0.0291**
Yeast-2-vs-8	'Random_based'	0.7907±0.0759	0.7952±0.0865	0.2543±0.0871	0.7857±0.0909
	'MNESR_based'	0.9143±0.0274	0.7460±0.0657	0.3612±0.0908	0.7201±0.0788
	MNEFD_IE	**0.9792±0.0121**	**0.8696±0.0978**	**0.7532±0.1358**	**0.8547±0.1152**
Yeast4	'Random_based'	0.8294±0.0494	0.8653±0.0551	0.2738±0.0529	0.8607±0.0547

'MNESR_based'	0.8330±0.0611	**0.8661±0.0506**	0.2837±0.0652	**0.8645±0.0510**
MNEFD_IE	**0.9097±0.0142**	0.8209±0.0693	**0.3553±0.0457**	0.8122±0.0787

As shown in Table 3, the performance of the MNEFD_IE is generally significantly better than that of the 'Random_based' algorithm in terms of all four evaluation metrics. This indicates that the two types of envelope samples are helpful for improving model accuracy. In terms of the four evaluation metrics, 'MNESR_based' generally outperforms 'Random_based', which means that the neighboring envelope samples can effectively mine the neighbor relationship among samples, thereby improving the classification performance. At the same time, MNEFD_IE generally achieves significant improvement compared with 'MNESR_based' in terms of four evaluation metrics, which means that the neighboring cluster envelope samples produced by CFCMD are more effective.

In addition, the diversity and performance of the base classifiers in the algorithms are also analyzed based on the Kappa-error diagram. Fig. 7 shows the diversity performance of the base classifiers obtained using MNEFD_IE, SMOTE Bagging, and Under Bagging algorithms on three datasets with different imbalance ratios. Among them, 'Neighboring samples based' means that the base classifiers are trained on the neighboring envelope samples. 'Hierarchical samples based' means that the base classifiers are trained on the neighboring cluster envelope samples.
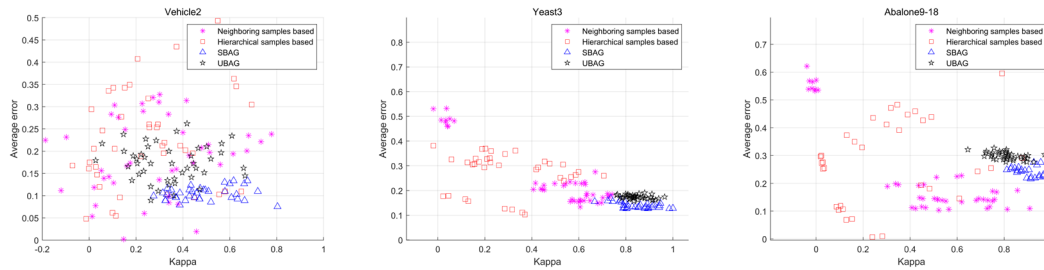
Fig. 7. Diversity and performance analysis of base classifiers

As shown in Fig. 7, MNEFD_IE can obtain data points with smaller Kappa values and average errors compared to the other two classical ensemble algorithms. This means that the base classifiers obtained by MNEFD_IE produce greater diversity and performance. Moreover, the Kappa values of data points obtained by 'Hierarchical samples based' are generally smaller than that of 'Neighboring samples based'. The possible reason for this is that the neighboring cluster envelope samples are obtained based on the neighboring envelope samples, and include the local and global structural information.

2.4. Algorithm comparison
2.4.1. Comparison with classical imbalanced ensemble algorithms
The proposed MNEFD_IE is compared with seven classical imbalanced ensemble algorithms for verification: SMOTE Bagging, Under Bagging, SMOTE Boost, RUSBoost, EUSBoost, Balance Cascade, and Easy Ensemble.

The details and parameter settings of the classical ensemble learning algorithms are shown in subsection 'Experimental Conditions'. The results are shown in Table 4. The last row of Table 4 shows the percentage of each algorithm achieving the best performance among the compared algorithms based on 38 datasets and 4 evaluation metrics.

Table 4. Comparison with classical imbalanced ensemble algorithms

ID	Meas	SBAG	UBAG	SBO	RBO	EBO	BAC	Easy	MNEFD_

	ure								IE
1	ACC	0.7526± 0.0872	0.7430± 0.0882	0.8354± 0.0596	0.7663± 0.0717	0.7860± 0.0812	0.7055± 0.0693	0.6903± 0.0926	**0.9721± 0.0104**
	AUC	0.7400± 0.0747	0.7549± 0.0817	0.7839± 0.0652	0.7724± 0.0864	0.8013± 0.0695	0.7274± 0.0738	0.7127± 0.0962	**0.9662± 0.0011**
	F-M	0.6727± 0.0763	0.6903± 0.0807	0.7232± 0.0830	0.7043± 0.0911	0.7440± 0.0683	0.6599± 0.0703	0.6468± 0.0963	**0.9599± 0.0125**
	G-M	0.7364± 0.0728	0.7508± 0.0826	0.7767± 0.0659	0.7702± 0.0838	0.7979± 0.0745	0.7218± 0.0741	0.7079± 0.0957	**0.9656± 0.0011**
2	ACC	0.9648± 0.0095	0.9582± 0.0119	0.9648± 0.0141	0.9736± 0.0083	0.9546± 0.0141	0.9657± 0.0095	0.9619± 0.0119	**0.9898± 0.0083**
	AUC	0.9611± 0.0138	0.9609± 0.0112	0.9652± 0.0145	0.9739± 0.0111	0.9526± 0.0154	0.9473± 0.0132	0.9610± 0.0117	**0.9921± 0.0064**
	F-M	0.9501± 0.0138	0.9445± 0.0137	0.9506± 0.0196	0.9627± 0.0120	0.9358± 0.0194	0.9658± 0.0095	0.9463± 0.0166	**0.9857± 0.0115**
	G-M	0.9609± 0.0139	0.9607± 0.0114	0.9651± 0.0145	0.9738± 0.0113	0.9522± 0.0157	0.9619± 0.0095	0.9610± 0.0117	**0.9921± 0.0065**
3	ACC	0.7590± 0.0158	0.7214± 0.0408	0.7408± 0.0356	0.7356± 0.0309	0.7792± 0.0480	0.6901± 0.0307	0.7143± 0.0306	**0.8243± 0.0302**
	AUC	0.7274± 0.0155	0.7383± 0.0352	0.7291± 0.0529	0.7293± 0.0337	0.7566± 0.0392	0.7020± 0.0256	0.7124± 0.0423	**0.7954± 0.0343**
	F-M	0.6434± 0.0212	0.6666± 0.0356	0.6469± 0.0697	0.6511± 0.0414	0.6852± 0.0437	0.6252± 0.0277	0.6344± 0.0512	**0.7327± 0.0494**
	G-M	0.7196± 0.0165	0.7355± 0.0363	0.7257± 0.0575	0.7278± 0.0342	0.7541± 0.0379	0.6982± 0.0258	0.7114± 0.0423	**0.7823± 0.0460**
4	ACC	0.9866± 0.0182	0.9866± 0.0182	0.9933± 0.0149	0.9933± 0.0149	0.9933± 0.0149	**1±0**	0.9933± 0.0149	**1±0**
	AUC	0.9800± 0.0273	0.9800± 0.0273	0.9900± 0.0223	0.9900± 0.0223	0.9900± 0.0223	**1±0**	0.9900± 0.0223	**1±0**
	F-M	0.9789± 0.0288	0.9789± 0.0288	0.9894± 0.0235	0.9894± 0.0235	0.9894± 0.0235	**1±0**	0.9894± 0.0235	**1±0**
	G-M	0.9794± 0.0281	0.9794± 0.0281	0.9897± 0.0229	0.9897± 0.0229	0.9897± 0.0229	**1±0**	0.9897± 0.0229	**1±0**
5	ACC	0.7030± 0.0246	0.7263± 0.0239	0.7183± 0.0336	0.7398± 0.0253	0.6913± 0.0551	0.6440± 0.0433	0.6543± 0.0207	**0.7399± 0.0516**
	AUC	0.6924± 0.0239	0.7210± 0.0347	0.6946± 0.0280	0.7104± 0.0400	0.7081± 0.0307	0.6794± 0.0080	0.6752± 0.0144	**0.7397± 0.0239**
	F-M	0.5621± 0.0347	0.5989± 0.0418	0.5648± 0.0401	0.5864± 0.0522	0.5857± 0.0394	0.5885± 0.0456	0.5481± 0.0146	**0.6246± 0.0357**
	G-M	0.6855± 0.0331	0.7204± 0.0351	0.6865± 0.0366	0.7066± 0.0434	0.7032± 0.0304	0.6696± 0.0192	0.6728± 0.0156	**0.7366± 0.0211**
6	ACC	0.6532± 0.0654	0.6598± 0.0565	0.6370± 0.0473	0.6575± 0.0641	0.7018± 0.0427	0.6172± 0.0830	0.6843± 0.0758	**0.9905± 0.0130**
	AUC	0.6304±	0.6422±	0.6145±	0.6639±	0.6548±	0.6210±	0.6008±	**0.9947±**

		0.0521	0.0476	0.0540	0.0376	0.0647	0.0920	0.1185	**0.0072**
	F-M	0.4698± 0.0637	0.4861± 0.0640	0.4517± 0.0698	0.5076± 0.0488	0.4901± 0.0849	0.6581± 0.1180	0.3728± 0.2543	**0.9556± 0.0609**
	G-M	0.6208± 0.0463	0.6188± 0.0802	0.6096± 0.0572	0.6575± 0.0382	0.6375± 0.0719	0.6189± 0.0919	0.5165± 0.2490	**0.9947± 0.0073**
7	ACC	0.9621± 0.0130	0.9566± 0.0179	0.9657± 0.0188	0.9621± 0.0184	**0.9704± 0.0200**	0.9515± 0.0153	0.9455± 0.0211	0.9503± 0.0456
	AUC	0.9525± 0.0245	0.9536± 0.0082	0.9661± 0.0140	0.9671± 0.0206	**0.9681± 0.0210**	0.9539± 0.0050	0.9559± 0.0176	0.9606± 0.0313
	F-M	0.9270± 0.0261	0.9235± 0.0320	0.9328± 0.0375	0.9304± 0.0340	**0.9442± 0.0373**	0.9114± 0.0241	0.9031± 0.0352	0.9148± 0.0694
	G-M	0.9532± 0.0244	0.9599± 0.0175	0.9660± 0.0140	0.9669± 0.0206	**0.9680± 0.0212**	0.9536± 0.0051	0.9555± 0.0178	0.9599± 0.0325
8	ACC	0.7677± 0.0092	0.7411± 0.0234	0.7718± 0.0287	0.7564± 0.0295	0.7494± 0.0343	0.7055± 0.0446	0.7257± 0.0351	**0.8120± 0.0383**
	AUC	0.7618± 0.0170	0.7768± 0.0235	0.7441± 0.0348	0.7493± 0.0545	**0.7902± 0.0315**	0.7360± 0.0400	0.7386± 0.0360	0.7870± 0.0509
	F-M	0.6190± 0.0195	0.6213± 0.0265	0.6015± 0.0423	0.5993± 0.0643	0.6364± 0.0377	0.5765± 0.0459	0.5830± 0.0420	**0.6601± 0.0586**
	G-M	0.7613± 0.0177	0.7720± 0.0219	0.7402± 0.0386	0.7464± 0.0584	**0.7854± 0.0312**	0.7314± 0.0391	0.7377± 0.0362	0.7785± 0.0612
9	ACC	0.9203± 0.0487	0.8831± 0.0520	0.9392± 0.0390	0.9203± 0.0428	0.9161± 0.0533	0.9157± 0.0359	0.9219± 0.0268	**0.9953± 0.0104**
	AUC	0.9198± 0.0466	0.8885± 0.0503	0.9185± 0.0514	0.9269± 0.0324	0.9101± 0.0514	0.8892± 0.0517	0.9171± 0.0313	**0.9970± 0.0068**
	F-M	0.8509± 0.0872	0.7903± 0.0863	0.8730± 0.0807	0.8529± 0.0740	0.8414± 0.0880	0.8255± 0.0715	0.8536± 0.0521	**0.9905± 0.0213**
	G-M	0.9183± 0.0465	0.8862± 0.0491	0.9171± 0.0524	0.9258± 0.0322	0.9078± 0.0522	0.9054± 0.0435	0.9159± 0.0319	**0.9969± 0.0068**
10	ACC	0.9337± 0.0215	0.9349± 0.0131	0.9396± 0.0252	0.9550± 0.0106	0.9397± 0.0234	0.9255± 0.0239	0.9302± 0.0224	**0.9657± 0.0190**
	AUC	0.9359± 0.0308	0.9523± 0.0189	0.9311± 0.0385	0.9618± 0.0138	0.9466± 0.0279	0.9356± 0.0223	0.9370± 0.0312	**0.9655± 0.0118**
	F-M	0.8703± 0.0416	0.8769± 0.0251	0.8768± 0.0519	0.9108± 0.0206	0.8827± 0.0440	0.8588± 0.0393	0.8652± 0.0418	**0.9311± 0.0349**
	G-M	0.9355± 0.0311	0.9516± 0.0187	0.9305± 0.0389	0.9617± 0.0137	0.9465± 0.0278	0.9353± 0.0225	0.9365± 0.0315	**0.9652± 0.0119**
11	ACC	0.8814± 0.0376	0.8721± 0.0540	0.8840± 0.0436	0.8839± 0.0266	0.8750± 0.0734	0.8600± 0.0584	0.8481± 0.0611	**0.9910± 0.0082**
	AUC	0.8998± 0.0196	0.8990± 0.0501	0.8474± 0.0587	0.9068± 0.0290	0.8918± 0.0578	0.8637± 0.0439	0.8698± 0.0564	**0.9800± 0.0183**
	F-M	0.7865± 0.0489	0.7777± 0.0761	0.7562± 0.0916	0.7908± 0.0348	0.7820± 0.0953	0.7475± 0.0773	0.7383± 0.0855	**0.9793± 0.0189**
	G-M	0.8975±	0.8961±	0.8436±	0.9042±	0.8878±	0.8616±	0.8666±	**0.9797±**

		0.0187	0.0510	0.0621	0.0289	0.0616	0.0434	0.0570	**0.0186**
12	ACC	0.9168±	0.8929±	0.9346±	0.9046±	0.8990±	0.8539±	0.8212±	**0.9761±**
		0.0379	0.0408	0.0301	0.0252	0.0570	0.0376	0.0427	**0.0257**
	AUC	0.8926±	0.8899±	0.9090±	0.8905±	0.8862±	0.8670±	0.8485±	**0.9538±**
		0.0721	0.0353	0.0786	0.0332	0.0639	0.0341	0.0298	**0.0291**
	F-M	0.7606±	0.7247±	0.8023±	0.7408±	0.7357±	0.6552±	0.6095±	**0.9242±**
		0.1042	0.0834	0.0962	0.0364	0.1204	0.0653	0.0525	**0.0787**
	G-M	0.8870±	0.8897±	0.9054±	0.8878±	0.8857±	0.8653±	0.8459±	**0.9532±**
		0.0744	0.0353	0.0842	0.0356	0.0645	0.0332	0.0284	**0.0293**
13	ACC	0.9346±	0.8972±	0.9345±	0.9108±	0.8877±	0.8875±	0.8550±	**0.9766±**
		0.0191	0.0421	0.0106	0.0518	0.0894	0.0395	0.0387	**0.0233**
	AUC	0.8923±	0.9159±	0.8504±	0.9227±	0.8932±	0.8932±	0.8463±	**0.9586±**
		0.0965	0.0576	0.0815	0.0342	0.0700	0.0359	0.0935	**0.0709**
	F-M	0.7657±	0.7159±	0.7447±	0.7507±	0.7121±	0.6893±	0.6050±	**0.9132±**
		0.1005	0.0953	0.0615	0.1082	0.1598	0.0791	0.1065	**0.0881**
	G-M	0.8836±	0.9115±	0.8353±	0.9182±	0.8912±	0.8913±	0.8390±	**0.9551±**
		0.1123	0.0553	0.0970	0.0340	0.0701	0.0352	0.1036	**0.0783**
14	ACC	0.9413±	0.9279±	0.9386±	0.9225±	0.9198±	0.9076±	0.9130±	**0.9905±**
		0.0218	0.0258	0.0086	0.0263	0.0252	0.0257	0.0222	**0.0130**
	AUC	0.9401±	0.9353±	0.8795±	0.9188±	0.9281±	0.9079±	0.9109±	**0.9947±**
		0.0197	0.0155	0.0148	0.0240	0.0166	0.0316	0.0274	**0.0072**
	F-M	0.7822±	0.7472±	0.7427±	0.7260±	0.7244±	0.6871±	0.6989±	**0.9556±**
		0.0661	0.0673	0.0290	0.0698	0.0597	0.0697	0.0580	**0.0609**
	G-M	0.9401±	0.9350±	0.8761±	0.9188±	0.9277±	0.9079±	0.9108±	**0.9947±**
		0.0197	0.0156	0.0157	0.0240	0.0168	0.0316	0.0274	**0.0073**
15	ACC	0.8898±	0.8424±	0.9107±	0.8720±	0.8621±	0.8090±	0.8451±	**0.9628±**
		0.0227	0.0520	0.0179	0.0522	0.0174	0.1216	0.0822	**0.0584**
	AUC	0.8754±	0.8994±	0.8744±	0.8402±	0.8605±	0.8112±	0.8504±	**0.9442±**
		0.0467	0.0386	0.0735	0.0332	0.0746	0.0749	0.0463	**0.0516**
	F-M	0.6197±	0.5710±	0.6563±	0.5778±	0.5621±	0.4820±	0.5544±	**0.8806±**
		0.0525	0.0843	0.0814	0.0686	0.0549	0.1089	0.0845	**0.1533**
	G-M	0.8736±	0.8955±	0.8693±	0.8346±	0.8552±	0.7996±	0.8439±	**0.9413±**
		0.0481	0.0396	0.0823	0.0337	0.0810	0.0831	0.0493	**0.0544**
16	ACC	0.9163±	0.9124±	0.9435±	0.9299±	0.9144±	0.9066±	0.9046±	**0.9845±**
		0.0108	0.0305	0.0187	0.0371	0.0510	0.0520	0.0221	**0.0128**
	AUC	0.8910±	0.9335±	0.8893±	0.9263±	0.9267±	0.8866±	0.9212±	**0.9833±**
		0.0753	0.0229	0.0455	0.0296	0.0196	0.0358	0.0433	**0.0251**
	F-M	0.6664±	0.6914±	0.7428±	0.7342±	0.7024±	0.6632±	0.6642±	**0.9286±**
		0.0600	0.0662	0.0829	0.0819	0.1029	0.0875	0.0618	**0.0532**
	G-M	0.8861±	0.9324±	0.9058±	0.9247±	0.9253±	0.8827±	0.9199±	**0.9832±**
		0.0830	0.0229	0.0581	0.0309	0.0209	0.0396	0.0435	**0.0253**
17	ACC	0.8541±	0.7916±	0.8900±	0.8351±	0.8180±	0.7557±	0.8047±	**0.9263±**
		0.0340	0.0179	0.0321	0.0295	0.0324	0.0313	0.0516	**0.0039**
	AUC	0.8217±	0.7969±	0.7727±	0.7862±	0.8206±	0.7511±	0.7801±	**0.9235±**

Group	Metric								
		0.0822	0.0385	0.0907	0.0899	0.0471	0.0658	0.0640	**0.0779**
	F-M	0.5089±0.1030	0.4271±0.0403	0.5235±0.1359	0.4581±0.0987	0.4692±0.0679	0.3686±0.0432	0.4298±0.0675	**0.6977±0.0370**
	G-M	0.8165±0.0885	0.7963±0.0386	0.7523±0.1114	0.7788±0.0982	0.8197±0.0473	0.7456±0.0636	0.7757±0.0693	**0.9184±0.0873**
18	ACC	0.8331±0.0475	0.6667±0.0261	0.8491±0.0423	0.7809±0.0607	0.7182±0.0896	0.6300±0.1074	0.6345±0.1013	**0.9795±0.0115**
	AUC	0.6676±0.1698	0.7035±0.1160	0.6014±0.1304	0.6999±0.1416	0.7930±0.1055	0.6254±0.1762	0.7390±0.1278	**0.9000±0.0559**
	F-M	0.4020±0.1666	0.2771±0.0862	0.3234±0.1658	0.3196±0.1500	0.3669±0.1032	0.2199±0.0984	0.3066±0.1166	**0.8857±0.0639**
	G-M	0.5605±0.3434	0.6863±0.1213	0.4569±0.2871	0.6692±0.1733	0.7851±0.1015	0.5965±0.1821	0.7259±0.1226	**0.8928±0.0599**
19	ACC	0.8174±0.0518	0.5888±0.0579	0.8594±0.0585	0.7662±0.1562	0.7053±0.0626	0.5750±0.1166	0.5933±0.1077	**0.9814±0.0104**
	AUC	0.7019±0.1399	0.7766±0.0316	0.7330±0.0945	0.6375±0.1506	0.7646±0.0711	0.6174±0.1515	0.7795±0.0565	**0.8607±0.0745**
	F-M	0.3847±0.1180	0.2796±0.0375	0.4141±0.1420	0.3190±0.2350	0.3129±0.0714	0.2064±0.0854	0.2903±0.0845	**0.8400±0.0894**
	G-M	0.6077±0.3421	0.7428±0.0422	0.7114±0.1150	0.6110±0.1610	0.7569±0.0638	0.6134±0.1478	0.7445±0.0766	**0.8532±0.0821**
20	ACC	0.8237±0.0556	0.7363±0.0262	0.8065±0.0742	**0.8257±0.0558**	0.7996±0.0336	0.6404±0.0785	0.6817±0.0821	0.8110±0.0531
	AUC	0.7208±0.0367	0.6883±0.0798	0.7259±0.0319	0.7827±0.0943	0.7222±0.1005	0.6526±0.1016	0.7212±0.0346	**0.8214±0.0294**
	F-M	0.3174±0.0480	0.2361±0.0525	0.3142±0.0662	0.3601±0.0813	0.2946±0.0899	0.1974±0.0634	0.2425±0.0201	**0.3732±0.0614**
	G-M	0.7074±0.0455	0.6778±0.0981	0.7170±0.0356	0.7749±0.1005	0.7105±0.1192	0.6425±0.1109	0.7113±0.0416	**0.8210±0.0291**
21	ACC	0.9060±0.0610	0.8773±0.0577	0.9343±0.0355	0.9018±0.0665	0.8975±0.1390	0.8036±0.0881	0.8693±0.0706	**0.9902±0.0134**
	AUC	0.9025±0.0885	0.8593±0.1031	0.8866±0.1011	0.9004±0.1392	0.8666±0.1520	0.8480±0.1249	0.8208±0.1130	**0.9949±0.0070**
	F-M	0.5733±0.1382	0.4666±0.1027	0.6189±0.1166	0.5563±0.2347	0.6187±0.2352	0.3915±0.2176	0.4389±0.1094	**0.9200±0.1095**
	G-M	0.8921±0.1066	0.8487±0.1153	0.8749±0.1178	0.8962±0.1469	0.8578±0.1610	0.8393±0.1301	0.8108±0.1214	**0.9948±0.0071**
22	ACC	0.9524±0.0193	0.8363±0.0802	0.9582±0.0164	0.8927±0.0867	0.8600±0.1016	0.8539±0.0492	0.8869±0.0248	**0.9911±0.0081**
	AUC	0.8810±0.0497	0.8427±0.0773	0.8373±0.0964	0.8961±0.0714	0.9021±0.1029	0.8989±0.0593	0.8930±0.0531	**0.9953±0.0043**
	F-M	0.7463±0.1452	0.4118±0.1298	0.6666±0.1020	0.5680±0.2540	0.5121±0.2370	0.4491±0.1020	0.4888±0.0248	**0.9333±0.0609**
	G-M	0.8753±	0.8394±	0.8177±	0.8920±	0.9005±	0.8956±	0.8897±	**0.9952±**

		0.0523	0.0756	0.1151	0.0737	0.1026	0.0596	0.0541	**0.0043**
23	ACC	0.8617± 0.0601	0.7369± 0.0566	0.9137± 0.0458	0.8002± 0.0353	0.7523± 0.0597	0.7358± 0.0713	0.6880± 0.0665	**0.9623± 0.0048**
	AUC	0.7257± 0.1537	0.7819± 0.0526	0.7533± 0.1430	0.7906± 0.0992	0.7326± 0.0941	0.7502± 0.1094	0.7220± 0.0595	**0.9212± 0.0807**
	F-M	0.3392± 0.1904	0.2755± 0.0453	0.4560± 0.2876	0.3146± 0.0807	0.2504± 0.0572	0.2628± 0.0932	0.2257± 0.0444	**0.7166± 0.0151**
	G-M	0.6932± 0.1850	0.7770± 0.0536	0.7149± 0.1897	0.7834± 0.1052	0.7196± 0.1073	0.7463± 0.1094	0.7165± 0.0586	**0.9173± 0.0859**
24	ACC	0.9221± 0.0109	0.9384± 0.0842	0.9340± 0.0241	0.9692± 0.0688	**1±0**	**1±0**	**1±0**	**1±0**
	AUC	0.9558± 0.0077	0.9473± 0.0447	0.9114± 0.0904	0.9840± 0.0357	**1±0**	**1±0**	**1±0**	**1±0**
	F-M	0.6334± 0.0383	0.7666± 0.3248	0.6269± 0.0362	0.8666± 0.2981	**1±0**	**1±0**	**1±0**	**1±0**
	G-M	0.9551± 0.0076	0.9658± 0.0467	0.9027± 0.1095	0.9833± 0.0373	**1±0**	**1±0**	**1±0**	**1±0**
25	ACC	0.9488± 0.0382	0.9495± 0.0310	0.9673± 0.0126	0.8976± 0.0879	0.9297± 0.0572	0.9018± 0.0476	0.9390± 0.0538	**0.9884± 0.0164**
	AUC	0.9256± 0.0998	0.5266± 0.2712	0.9353± 0.1037	0.9463± 0.0461	0.9634± 0.0298	0.9487± 0.0249	0.9682± 0.0280	**0.9939± 0.0086**
	F-M	0.6619± 0.1980	**0.9512± 0.0298**	0.6933± 0.0596	0.5815± 0.3015	0.6066± 0.2832	0.4866± 0.1849	0.6266± 0.2385	0.9000± 0.1414
	G-M	0.9164± 0.1185	0.9065± 0.0569	0.9266± 0.1228	0.9438± 0.0487	0.9623± 0.0310	0.9471± 0.0261	0.9674± 0.0292	**0.9939± 0.0087**
26	ACC	0.9584± 0.0181	0.7590± 0.1437	0.9646± 0.0174	0.9335± 0.0059	0.7820± 0.0375	0.6823± 0.0972	0.7637± 0.0961	**0.9792± 0.0121**
	AUC	0.8109± 0.1566	0.7307± 0.1349	0.7902± 0.1070	0.8457± 0.0030	0.7666± 0.0844	0.7625± 0.1149	0.7571± 0.1331	**0.8696± 0.0978**
	F-M	0.5473± 0.1410	0.2327± 0.1257	0.5833± 0.1666	0.4846± 0.0210	0.2238± 0.0514	0.1910± 0.0758	0.2214± 0.0736	**0.7532± 0.1358**
	G-M	0.7697± 0.2034	0.7215± 0.1378	0.7528± 0.1564	0.8403± 0.0027	0.7613± 0.0878	0.7485± 0.1142	0.7471± 0.1340	**0.8547± 0.1152**
27	ACC	0.7978± 0.0482	0.7742± 0.0275	0.8215± 0.0885	0.8200± 0.0347	0.8126± 0.0403	0.7850± 0.0532	0.7998± 0.0588	**0.9097± 0.0142**
	AUC	0.8339± 0.0374	**0.8452± 0.0970**	0.7979± 0.0779	0.8199± 0.0472	0.8372± 0.0611	0.7747± 0.0966	0.8191± 0.0865	0.8209± 0.0693
	F-M	0.2345± 0.0278	0.2097± 0.0219	0.2466± 0.0488	0.2398± 0.0170	0.2437± 0.0397	0.2031± 0.0592	0.2337± 0.0750	**0.3553± 0.0457**
	G-M	0.8307± 0.0327	0.8179± 0.0717	0.7835± 0.0916	0.8165± 0.0462	**0.8340± 0.0594**	0.7710± 0.1002	0.8159± 0.0880	0.8122± 0.0781
28	ACC	0.8930± 0.0156	0.6897± 0.0454	0.9392± 0.0047	0.8116± 0.0324	0.7535± 0.0876	0.6113± 0.0831	0.6611± 0.1143	**0.9677± 0.0018**
	AUC	0.6523±	**0.6666±**	0.5867±	0.6228±	0.6110±	0.6500±	0.6403±	0.6034±

		0.0732	**0.0750**	0.0582	0.0453	0.0788	0.0791	0.0669	0.1003
	F-M	0.1970±0.0716	0.1206±0.0285	0.2180±0.0403	0.1330±0.0335	0.1051±0.0124	0.1021±0.0186	0.1083±0.0217	**0.2699±0.1787**
	G-M	0.5921±0.1039	**0.6600±0.0797**	0.3999±0.2266	0.5879±0.0552	0.5630±0.1616	0.6335±0.0727	0.6206±0.0824	0.4239±0.2120
29	ACC	0.8253±0.0177	0.7285±0.0661	0.8171±0.0096	0.8456±0.0239	0.7696±0.0990	0.6472±0.0484	0.5957±0.1497	**0.8468±0.0976**
	AUC	0.6711±0.1485	0.7147±0.0517	0.7299±0.1313	0.7389±0.0896	0.6714±0.0611	0.6727±0.0260	0.6783±0.0562	**0.8000±0.0066**
	F-M	0.1498±0.0788	0.1423±0.0212	0.1851±0.0714	0.1992±0.0365	0.1440±0.0471	0.1122±0.0093	0.1130±0.0231	**0.2628±0.0997**
	G-M	0.6200±0.2011	0.7089±0.0561	0.7065±0.1625	0.7191±0.1208	0.6537±0.0801	0.6702±0.0229	0.6591±0.0712	**0.7954±0.0137**
30	ACC	0.9703±0.0122	0.9393±0.0189	**0.9757±0.0087**	0.9440±0.1475	0.9602±0.0096	0.9333±0.0197	0.9198±0.0191	0.9636±0.0140
	AUC	**0.9618±0.0320**	0.9458±0.0293	0.9444±0.0555	0.9604±0.0282	0.9458±0.0308	0.9534±0.0220	0.9479±0.0223	0.9597±0.0291
	F-M	0.6669±0.0925	0.4917±0.0811	**0.7018±0.0541**	0.5158±0.0678	0.5849±0.0624	0.4736±0.0642	0.4253±0.0464	0.6231±0.0788
	G-M	**0.9612±0.0325**	0.9451±0.0294	0.9418±0.0589	0.9600±0.0282	0.9452±0.0312	0.9526±0.0221	0.9470±0.0222	0.9592±0.0295
31	ACC	0.9521±0.0114	0.8679±0.0335	**0.9676±0.0084**	0.8746±0.0377	0.8712±0.0517	0.7776±0.0334	0.7755±0.0493	0.9137±0.0173
	AUC	0.8360±0.1076	0.8766±0.0594	0.7743±0.1489	0.8382±0.0795	0.8225±0.1086	0.8162±0.0426	0.8293±0.0513	**0.8868±0.0170**
	F-M	0.4103±0.0799	0.2466±0.0502	**0.4407±0.1667**	0.2353±0.0390	0.2206±0.0575	0.1548±0.0158	0.1603±0.0266	0.3234±0.0472
	G-M	0.8179±0.1288	0.8746±0.0593	0.7252±0.1973	0.8307±0.0848	0.8135±0.1236	0.8135±0.0405	0.8246±0.0488	**0.8861±0.0175**
32	ACC	0.9333±0.0143	0.7411±0.0529	0.9518±0.0032	0.7866±0.0873	0.7688±0.0550	0.7069±0.0517	0.5966±0.1318	**0.9889±0.0045**
	AUC	0.6605±0.0675	0.7698±0.0618	0.7310±0.1207	0.7198±0.1365	0.7107±0.1565	0.7279±0.1075	0.6715±0.0420	**0.8111±0.0722**
	F-M	0.1980±0.0557	0.1237±0.0255	0.3025±0.1000	0.1347±0.0713	0.1176±0.0589	0.1043±0.0323	0.0779±0.0115	**0.7113±0.1216**
	G-M	0.5865±0.1133	0.7674±0.0581	0.6772±0.1771	0.7101±0.1409	0.6940±0.1782	0.7223±0.1054	0.6521±0.0527	**0.7855±0.0916**
33	ACC	0.9005±0.0354	0.6596±0.0886	**0.9502±0.0139**	0.8070±0.0423	0.6830±0.1012	0.6783±0.1094	0.6549±0.0726	0.8302±0.1735
	AUC	0.7349±0.0847	0.7446±0.0555	0.7298±0.1264	0.7139±0.1216	0.6750±0.0523	0.7625±0.1077	0.6933±0.1589	**0.9136±0.0082**
	F-M	0.1937±0.0712	0.0956±0.230	**0.2955±0.1582**	0.1151±0.0452	0.0813±0.0108	0.1043±0.0379	0.0819±0.0382	0.2679±0.2273
	G-M	0.7054±	0.7323±	0.6764±	0.6886±	0.6610±	0.7467±	0.6748±	**0.9069±**

Group	Metric								
		0.1165	0.0490	0.1776	0.1536	0.0447	0.1106	0.1727	**0.0974**
34	ACC	0.9294±0.0140	0.8376±0.0610	0.9374±0.0122	0.8945±0.0467	0.9095±0.0337	0.8362±0.0679	0.8602±0.0333	**0.9932±0.0080**
	AUC	0.9564±0.0120	0.8779±0.0683	0.9177±0.0611	0.9462±0.0238	0.9539±0.0172	0.9165±0.0347	0.8732±0.0909	**0.9965±0.0041**
	F-M	0.6436±0.0659	0.1802±0.0277	0.6434±0.0661	0.2836±0.0897	0.3081±0.0860	0.1970±0.0545	0.1979±0.0683	**0.8684±0.0239**
	G-M	0.9562±0.0118	0.8704±0.0744	0.9151±0.0642	0.9444±0.0252	0.9526±0.0180	0.9128±0.0391	0.8693±0.0940	**0.9965±0.0041**
35	ACC	**1±0**	**1±0**	**1±0**	0.9834±0.0371	**1±0**	**1±0**	**1±0**	**1±0**
	AUC	**1±0**	**1±0**	**1±0**	0.9915±0.0188	**1±0**	**1±0**	**1±0**	**1±0**
	F-M	**1±0**	**1±0**	**1±0**	0.8533±0.3279	**1±0**	**1±0**	**1±0**	**1±0**
	G-M	**1±0**	**1±0**	**1±0**	0.9913±0.0192	**1±0**	**1±0**	**1±0**	**1±0**
36	ACC	0.9996±0.0010	0.9861±0.0168	0.9986±0.0020	0.9605±0.0232	0.9852±0.0201	0.9771±0.0223	0.9520±0.0078	**1±0**
	AUC	0.9833±0.0373	0.9929±0.0085	0.9828±0.0370	0.9800±0.0117	0.9760±0.0345	0.9884±0.0113	0.9757±0.0039	**1±0**
	F-M	0.9818±0.0407	0.7471±0.2704	0.9532±0.0666	0.4848±0.2898	0.7387±0.2556	0.6533±0.3207	0.3622±0.0357	**1±0**
	G-M	0.9826±0.0390	0.9929±0.0086	0.9821±0.0387	0.9797±0.0119	0.9752±0.0361	0.9882±0.0114	0.9754±0.0041	**1±0**
37	ACC	0.9694±0.0142	0.9334±0.0196	0.9660±0.0153	0.9402±0.0347	0.9544±0.0340	0.9366±0.0292	0.9357±0.0235	**0.9995±0.0010**
	AUC	0.9570±0.0492	0.9662±0.0099	0.9462±0.0542	0.9697±0.0176	0.9769±0.0172	0.9679±0.0148	0.9674±0.0119	**0.9833±0.0622**
	F-M	0.7258±0.0399	0.2830±0.0757	0.7178±0.0448	0.3391±0.1441	0.4431±0.2470	0.3257±0.1712	0.2950±0.0914	**0.9818±0.0407**
	G-M	0.9553±0.0523	0.9656±0.0102	0.9439±0.0577	0.9691±0.0181	0.9765±0.0176	0.9672±0.0151	0.9668±0.0122	**0.9826±0.0390**
38	ACC	0.9854±0.0644	0.9825±0.0279	0.9858±0.0290	0.9818±0.0283	0.9829±0.0282	0.9863±0.0292	0.9784±0.0266	**0.9991±0.0012**
	AUC	0.9543±0.0621	0.9115±0.0506	0.9545±0.0623	0.9327±0.0620	0.9315±0.0631	0.9547±0.0625	0.9094±0.0514	**0.9550±0.0622**
	F-M	0.8769±0.1315	0.8420±0.1243	0.8987±0.1244	0.8057±0.2371	0.8642±0.1432	0.9169±0.1327	0.7531±0.2110	**0.9492±0.0705**
	G-M	0.9525±0.0644	0.9073±0.0528	0.9528±0.0646	0.9300±0.0643	0.9285±0.0658	**0.9530±0.0648**	0.9055±0.0535	0.9521±0.0664
Performance	ACC	1/38	1/38	4/38	1/38	3/38	3/38	2/38	**32/38**
	AUC	2/38	3/38	1/38	0/38	4/38	3/38	2/38	**32/38**
	F-M	1/38	2/38	4/38	0/38	3/38	3/38	2/38	**32/38**

G-M	2/38	2/38	1/38	0/38	5/38	3/38	3/38	**31/38**

As shown in the above table, the proposed MNEFD_IE achieves the best performance on more than 30 datasets. It generally shows a significant improvement in each evaluation metric compared to the classical imbalanced ensemble algorithms. For example, MNEFD_IE obtains the best performance on Kr-vs-k-zero_vs_eight with the mean ACC, AUC, F-M, and G-M results of 0.9932, 0.9965, 0.8684, and 0.9965, which are 5.58%, 4.01%, 22.48%, and 4.03% better than the second-best results, respectively. It means that the structural information among samples and high-quality envelope samples produced by MNEFD_IE is effective in improving the classification performance.

The average rankings of all compared algorithms on different evaluation metrics based on the Friedman aligned rank test are given to estimate the performance of MNEFD_IE. Fig. 8 shows the average rank numbers of the proposed algorithm and the other seven classical imbalanced ensemble algorithms based on 38 datasets, where lower rank number indicates better classification ability.
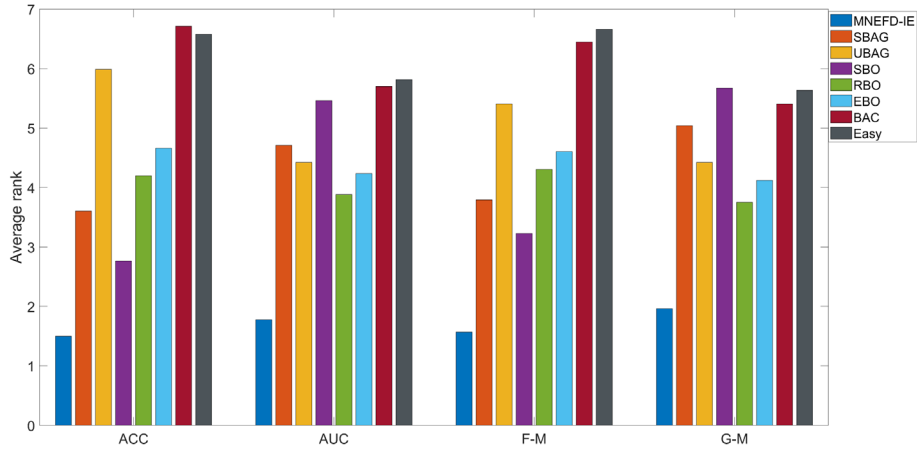
Fig. 8. Average ranks of all compared ensemble methods

As shown in Fig. 8, the average rank numbers of the other compared algorithms for the four metrics are significantly worse than those of MNEFD_IE. Therefore, the proposed algorithm MNEFD_IE outperforms the classical imbalanced ensemble algorithms apparently.

The performance of MNEFD_IE was further evaluated using Holm's test. The results are shown in Table 5 by setting the MNEFD_IE as a control algorithm, thus further analyzing whether there are significant differences between the proposed algorithm and the compared algorithms.

Table 5. P values from Holm's test

Algorithm	ACC	AUC	F-M	G-M	Hypothesis (0.05)
SBAG	1.4394e-07	9.8556e-10	1.8974e-08	8.1672e-12	**Rejected**
UBAG	2.2882e-27	5.0702e-09	4.4469e-20	1.3204e-08	**Rejected**
SBO	1.1707e-03	2.4488e-15	1.2966e-05	5.8939e-16	**Rejected**
RBO	1.7973e-11	3.3785e-06	2.7651e-11	1.9413e-05	**Rejected**
EBO	1.7601e-16	3.6705e-09	1.8417e-14	1.4852e-07	**Rejected**
BAC	1.5289e-35	7.6447e-18	2.7724e-30	9.4960e-15	**Rejected**
Easy	1.8088e-34	1.3937e-18	5.4957e-32	3.9370e-16	**Rejected**

As shown in Table 5, the equivalence hypotheses between MNEFD_IE and the compared algorithms are all rejected, which indicates significant differences between MNEFD_IE and the compared

algorithms at the significance level of 0.05. It means that the proposed algorithm is significantly better.

2.4.2. Comparison with state-of-the-art algorithms

To further verify the performance of the proposed MNEFD_IE, four state-of-the-art imbalanced ensemble algorithms were chosen: EASE, SPE, HUE, and ECUBoost. The specific results are shown in Table 6.

Table 6. The comparison results between EASE, SPE, HUE, ECUBoost and MNEFD_IE

ID	Measure	EASE	SPE	HUE	ECUBoost	MNEFD_IE
1	ACC	0.7756±0.0801	0.7754±0.0646	0.7942±0.0351	0.7620±0.0776	**0.9721±0.0104**
	AUC	0.7687±0.0901	0.7546±0.0679	0.7872±0.0430	0.7543±0.0821	**0.9662±0.0011**
	F-M	0.7008±0.1109	0.6845±0.0901	0.7238±0.0462	0.6849±0.0934	**0.9599±0.0125**
	G-M	0.7668±0.0911	0.7509±0.0694	0.7848±0.0426	0.7511±0.0816	**0.9656±0.0011**
2	ACC	0.9326±0.0224	0.9238±0.0149	0.9253±0.0202	0.9385±0.0228	**0.9898±0.0083**
	AUC	0.9337±0.0234	0.9154±0.0055	0.9262±0.0182	0.9401±0.0218	**0.9921±0.0064**
	F-M	0.9072±0.0303	0.8915±0.0150	0.8975±0.0255	0.9154±0.0308	**0.9857±0.0115**
	G-M	0.9335±0.0234	0.9140±0.0057	0.9259±0.0183	0.9399±0.0218	**0.9921±0.0065**
3	ACC	0.6523±0.0306	0.6470±0.0277	0.6588±0.0338	0.6745±0.0314	**0.8243±0.0302**
	AUC	0.6474±0.0297	0.6335±0.0344	0.6419±0.0339	0.6437±0.0312	**0.7954±0.0343**
	F-M	0.5590±0.0319	0.5372±0.0446	0.5455±0.0387	0.5357±0.0431	**0.7327±0.0494**
	G-M	0.6466±0.0297	0.6311±0.0359	0.6392±0.0339	0.6326±0.0367	**0.7823±0.0460**
4	ACC	**1±0**	**1±0**	**1±0**	**1±0**	**1±0**
	AUC	**1±0**	**1±0**	**1±0**	**1±0**	**1±0**
	F-M	**1±0**	**1±0**	**1±0**	**1±0**	**1±0**
	G-M	**1±0**	**1±0**	**1±0**	**1±0**	**1±0**
5	ACC	0.7358±0.0238	0.7237±0.0408	0.7243±0.0278	0.7385±0.0191	**0.7399±0.0516**
	AUC	0.7256±0.0244	0.7040±0.0357	0.7058±0.0278	0.7193±0.0161	**0.7397±0.0239**
	F-M	0.6054±0.0311	0.5804±0.0441	0.5818±0.0353	0.5986±0.0205	**0.6246±0.0357**
	G-M	0.7241±0.0248	0.7015±0.0355	0.7042±0.0280	0.7175±0.0162	**0.7366±0.0211**
6	ACC	0.6312±0.0802	0.5846±0.0690	0.5819±0.0796	0.4932±0.0634	**0.9905±0.0130**
	AUC	0.5877±0.0779	0.5823±0.0730	0.5339±0.0715	0.5519±0.0743	**0.9947±0.0072**
	F-M	0.4199±0.0827	0.4259±0.0793	0.3559±0.0764	0.4132±0.0719	**0.9556±0.0609**
	G-M	0.5792±0.0792	0.5807±0.0720	0.5188±0.0707	0.5327±0.0719	**0.9947±0.0073**
7	ACC	0.9645±0.0134	0.9645±0.0158	0.9538±0.0219	**0.9704±0.0106**	0.9503±0.0456
	AUC	0.9559±0.0189	0.9595±0.0166	0.9525±0.0178	**0.9636±0.0126**	0.9606±0.0313
	F-M	0.9257±0.0280	0.9328±0.0294	0.9149±0.0375	**0.9434±0.0183**	0.9148±0.0694
	G-M	0.9556±0.0191	0.9593±0.0167	0.9523±0.0178	**0.9632±0.0128**	0.9599±0.0325
8	ACC	0.7623±0.0278	0.7553±0.0079	0.7270±0.0374	0.7647±0.0285	**0.8120±0.0383**
	AUC	0.7281±0.0367	0.7206±0.0073	0.7333±0.0376	0.6860±0.0193	**0.7870±0.0509**
	F-M	0.5815±0.0494	0.5713±0.0100	0.5783±0.0438	0.5308±0.0293	**0.6601±0.0586**
	G-M	0.7242±0.0387	0.7168±0.0088	0.7311±0.0363	0.6672±0.0172	**0.7785±0.0612**
9	ACC	0.9346±0.0307	0.8967±0.0448	0.7270±0.0374	0.9345±0.0175	**0.9953±0.0104**
	AUC	0.9173±0.0380	0.8558±0.0552	0.7333±0.0376	0.9172±0.0419	**0.9970±0.0068**
	F-M	0.8668±0.0569	0.7840±0.0720	0.5783±0.0438	0.8640±0.0376	**0.9905±0.0213**
	G-M	0.9157±0.0391	0.8472±0.0607	0.7311±0.0363	0.9133±0.0461	**0.9969±0.0068**
10	ACC	0.9597±0.0196	0.9598±0.0137	0.9491±0.0087	0.9539±0.0195	**0.9657±0.0190**

	AUC	0.9545±0.0184	0.9459±0.0160	0.9581±0.0087	0.9542±0.0203	**0.9655±0.0118**
	F-M	0.9181±0.0376	0.9154±0.0267	0.9004±0.0162	0.9084±0.0357	**0.9311±0.0349**
	G-M	0.9544±0.0184	0.9451±0.0168	0.9579±0.0086	0.9535±0.0206	**0.9652±0.0119**
11	ACC	0.8989±0.0314	0.8841±0.0349	0.8571±0.0545	0.9136±0.0404	**0.9910±0.0082**
	AUC	0.8607±0.0500	0.8484±0.0653	0.8704±0.0412	0.8569±0.0625	**0.9800±0.0183**
	F-M	0.7802±0.0693	0.7524±0.0802	0.7476±0.0791	0.7981±0.0987	**0.9793±0.0189**
	G-M	0.8560±0.0536	0.8406±0.0732	0.8693±0.0418	0.8488±0.0684	**0.9797±0.0186**
12	ACC	0.9256±0.0523	0.9435±0.0303	0.8838±0.0176	0.8746±0.1476	**0.9761±0.0257**
	AUC	0.8871±0.0689	0.8942±0.0525	0.8846±0.0208	0.8575±0.0961	**0.9538±0.0291**
	F-M	0.7886±0.1235	0.8214±0.0922	0.7035±0.0223	0.7371±0.1897	**0.9242±0.0787**
	G-M	0.8840±0.0704	0.8895±0.0569	0.8831±0.0203	0.8454±0.1095	**0.9532±0.0293**
13	ACC	0.9486±0.0092	0.9439±0.0347	0.9302±0.0465	0.9485±0.0519	**0.9766±0.0233**
	AUC	0.9250±0.0623	0.8944±0.0963	0.9175±0.0435	0.9250±0.0669	**0.9586±0.0709**
	F-M	0.8197±0.0512	0.7921±0.1383	0.7967±0.1158	0.8387±0.1382	**0.9132±0.0881**
	G-M	0.9210±0.0676	0.8861±0.1090	0.9157±0.0441	0.9203±0.0721	**0.9551±0.0783**
14	ACC	0.9353±0.0062	0.9366±0.0157	0.9110±0.0208	0.9366±0.0152	**0.9905±0.0130**
	AUC	0.8826±0.0331	0.8810±0.0263	0.8964±0.0203	0.8969±0.0334	**0.9947±0.0072**
	F-M	0.7335±0.0327	0.7392±0.0576	0.6876±0.0478	0.7477±0.0422	**0.9556±0.0609**
	G-M	0.8791±0.0354	0.8779±0.0281	0.8955±0.0213	0.8942±0.0365	**0.9947±0.0073**
15	ACC	0.9078±0.0472	0.8986±0.0259	0.8572±0.0444	0.9195±0.0336	**0.9628±0.0584**
	AUC	0.8097±0.1166	0.7919±0.0953	0.8698±0.0447	0.8414±0.0921	**0.9442±0.0516**
	F-M	0.6100±0.1820	0.5695±0.1207	0.5736±0.0911	0.6571±0.1281	**0.8806±0.1533**
	G-M	0.7882±0.1378	0.7721±0.1094	0.8693±0.0443	0.8274±0.1096	**0.9413±0.0544**
16	ACC	0.9416±0.0261	0.9572±0.0131	0.8910±0.0187	0.9163±0.0265	**0.9845±0.0128**
	AUC	0.8623±0.0856	0.9316±0.0273	0.9047±0.0378	0.8661±0.0434	**0.9833±0.0251**
	F-M	0.7188±0.1360	0.8096±0.0486	0.6277±0.0546	0.6630±0.0430	**0.9286±0.0532**
	G-M	0.8517±0.0979	0.9302±0.0285	0.9037±0.0374	0.8594±0.0508	**0.9832±0.0253**
17	ACC	0.8806±0.0233	0.8599±0.0494	0.8086±0.0549	0.8977±0.0299	**0.9263±0.0039**
	AUC	0.8095±0.0620	0.8016±0.0910	0.7813±0.0486	0.7840±0.0367	**0.9235±0.0779**
	F-M	0.5387±0.0817	0.5109±0.1306	0.4440±0.1000	0.5538±0.0394	**0.6977±0.0370**
	G-M	0.8021±0.0676	0.7956±0.0947	0.7794±0.0493	0.7672±0.0488	**0.9184±0.0873**
18	ACC	0.7916±0.0600	0.7759±0.0543	0.6399±0.1113	0.6197±0.1118	**0.9795±0.0115**
	AUC	0.5700±0.0783	0.7054±0.1384	0.7059±0.0675	0.5061±0.1231	**0.9000±0.0559**
	F-M	0.2004±0.1249	0.2966±0.1573	0.2799±0.0489	0.1207±0.0815	**0.8857±0.0639**
	G-M	0.4436±0.2274	0.6121±0.3086	0.6843±0.0737	0.3878±0.2236	**0.8928±0.0599**
19	ACC	0.7944±0.0165	0.7849±0.0237	0.6966±0.0859	0.7988±0.0549	**0.9814±0.0104**
	AUC	0.7202±0.1439	0.6842±0.0887	0.7596±0.0851	0.7003±0.0758	**0.8607±0.0745**
	F-M	0.3147±0.1203	0.2911±0.0997	0.3145±0.0845	0.3233±0.0975	**0.8400±0.0894**
	G-M	0.6918±0.1640	0.6617±0.1144	0.7518±0.0819	0.6831±0.0928	**0.8532±0.0821**
20	ACC	0.8323±0.0389	0.7581±0.0205	0.6950±0.0887	**0.8583±0.0308**	0.8110±0.0531
	AUC	0.7088±0.0945	0.7001±0.0920	0.6663±0.1180	0.7537±0.0489	**0.8214±0.0294**
	F-M	0.2996±0.0735	0.2519±0.0564	0.2188±0.0905	0.3722±0.0445	**0.3732±0.0614**
	G-M	0.6767±0.1230	0.6888±0.0945	0.6430±0.1286	0.7390±0.0603	**0.8210±0.0291**
21	ACC	0.9486±0.0270	0.9486±0.0227	0.8321±0.0919	0.9627±0.0237	**0.9902±0.0134**

	AUC	0.8160±0.1426	0.8943±0.1058	0.8626±0.0873	0.9492±0.0710	**0.9949±0.0070**
	F-M	0.5895±0.2248	0.6599±0.1688	0.4204±0.1110	0.7690±0.1489	**0.9200±0.1095**
	G-M	0.7847±0.1711	0.8842±0.1187	0.8502±0.0989	0.9466±0.0759	**0.9948±0.0071**
22	ACC	0.9582±0.0274	0.9642±0.0223	0.8747±0.0515	0.9612±0.0152	**0.9911±0.0081**
	AUC	0.8373±0.1251	0.8873±0.0871	0.8865±0.1137	0.8623±0.1014	**0.9953±0.0043**
	F-M	0.6716±0.2234	0.7365±0.1263	0.4833±0.1598	0.6978±0.0939	**0.9333±0.0609**
	G-M	0.8096±0.1669	0.8756±0.1012	0.8808±0.1211	0.8436±0.1202	**0.9952±0.0043**
23	ACC	0.9083±0.0205	0.8768±0.0096	0.8371±0.0160	0.8617±0.0470	**0.9623±0.0048**
	AUC	0.7935±0.0862	0.7574±0.0591	0.7571±0.0417	0.7951±0.0890	**0.9212±0.0807**
	F-M	0.4554±0.1128	0.3636±0.0334	0.3202±0.0416	0.3780±0.0694	**0.7166±0.0151**
	G-M	0.7758±0.1065	0.7407±0.0688	0.7501±0.0469	0.7766±0.1180	**0.9173±0.0859**
24	ACC	**1±0**	0.9923±0.0153	**1±0**	0.9923±0.0153	**1±0**
	AUC	**1±0**	0.9000±0.2000	**1±0**	0.9500±0.0999	**1±0**
	F-M	**1±0**	0.8000±0.4000	**1±0**	0.9333±0.1333	**1±0**
	G-M	**1±0**	0.8000±0.4000	**1±0**	0.9414±0.1171	**1±0**
25	ACC	0.9812±0.0271	0.9812±0.0271	0.8788±0.0677	0.9112±0.0629	**0.9884±0.0164**
	AUC	0.8926±0.1968	0.9902±0.0142	0.9365±0.0356	0.9536±0.0330	**0.9939±0.0086**
	F-M	0.7142±0.3938	0.8476±0.1890	0.4504±0.1291	0.5454±0.2082	**0.9000±0.1414**
	G-M	0.7925±0.3965	0.9900±0.0144	0.9336±0.0382	0.9518±0.0348	**0.9939±0.0087**
26	ACC	0.9169±0.0287	0.8609±0.0267	0.7923±0.0579	0.8318±0.0444	**0.9792±0.0121**
	AUC	0.7653±0.0626	0.7600±0.1574	0.7959±0.0973	0.7448±0.0453	**0.8696±0.0978**
	F-M	0.3915±0.1006	0.2637±0.1019	0.2517±0.0684	0.2510±0.0470	**0.7532±0.1358**
	G-M	0.7433±0.0756	0.7180±0.2037	0.7895±0.0990	0.7334±0.0569	**0.8547±0.1152**
27	ACC	0.9083±0.0164	0.8712±0.0095	0.8167±0.0300	**0.9204±0.0229**	0.9097±0.0142
	AUC	0.7893±0.0782	0.8000±0.0392	0.8112±0.0534	0.8176±0.0429	**0.8209±0.0693**
	F-M	0.3316±0.0671	0.2791±0.0350	0.2351±0.0373	**0.3891±0.0734**	0.3553±0.0457
	G-M	0.7725±0.0917	0.7951±0.0437	0.8094±0.0520	0.8087±0.0485	**0.8122±0.0781**
28	ACC	0.7785±0.0302	0.7173±0.0542	0.6960±0.0204	0.6292±0.1777	**0.9677±0.0018**
	AUC	0.6124±0.0568	0.6168±0.0693	**0.6892±0.0451**	0.5906±0.0374	0.6034±0.1003
	F-M	0.1142±0.0266	0.1091±0.0345	0.1294±0.0156	0.0932±0.0192	**0.2699±0.1787**
	G-M	0.5779±0.0831	0.6010±0.0795	**0.6877±0.0459**	0.5529±0.0582	0.4239±0.2120
29	ACC	0.7877±0.0520	0.6980±0.0373	0.6737±0.0439	0.6737±0.1902	**0.8468±0.0976**
	AUC	0.6646±0.0267	0.6989±0.0447	0.6703±0.0719	0.7025±0.1043	**0.8000±0.0066**
	F-M	0.1424±0.0266	0.1274±0.0117	0.1129±0.0223	0.1559±0.0735	**0.2628±0.0997**
	G-M	0.6491±0.0288	0.6940±0.0469	0.6592±0.0845	0.6843±0.1096	**0.7954±0.0137**
30	ACC	**0.9770±0.0068**	0.9757±0.0107	0.9501±0.0100	0.9770±0.0077	0.9636±0.0140
	AUC	0.9006±0.0427	0.8892±0.0673	0.9513±0.0299	0.8885±0.0738	**0.9597±0.0291**
	F-M	**0.6854±0.0728**	0.6666±0.1285	0.5349±0.0514	0.6720±0.0938	0.6231±0.0788
	G-M	0.8956±0.0481	0.8815±0.0777	0.9509±0.0300	0.8794±0.0842	**0.9592±0.0295**
31	ACC	0.9420±0.0124	0.9103±0.0311	0.8786±0.0248	**0.9615±0.0083**	0.9137±0.0173
	AUC	0.8030±0.0698	0.8425±0.1048	0.8542±0.0245	0.8130±0.0597	**0.8868±0.0170**
	F-M	0.3509±0.0635	0.3038±0.0909	0.2482±0.0312	**0.4507±0.0919**	0.3234±0.0472
	G-M	0.7842±0.0874	0.8302±0.1192	0.8529±0.0265	0.7946±0.0768	**0.8861±0.0175**
32	ACC	0.9433±0.0214	0.8888±0.0312	0.8022±0.0191	0.6188±0.1883	**0.9889±0.0045**

	AUC	0.7511±0.1385	0.7232±0.0841	0.7034±0.0887	0.6829±0.0831	**0.8111±0.0722**
	F-M	0.2923±0.1600	0.1834±0.0531	0.1153±0.0293	0.1007±0.0560	**0.7113±0.1216**
	G-M	0.6427±0.3257	0.6890±0.1201	0.6816±0.1219	0.6595±0.0964	**0.7855±0.0916**
33	ACC	0.7964±0.0550	0.6257±0.0731	0.5918±0.0551	0.2350±0.1469	**0.8302±0.1735**
	AUC	0.5859±0.1207	0.6213±0.0944	0.6367±0.0701	0.5604±0.0913	**0.9136±0.0082**
	F-M	0.0732±0.0488	0.0623±0.0188	0.0638±0.0046	0.0480±0.0092	**0.2679±0.2273**
	G-M	0.4735±0.2590	0.5999±0.1044	0.6250±0.0588	0.4130±0.1613	**0.9069±0.0974**
34	ACC	0.9863±0.0075	0.9678±0.0073	0.9171±0.0135	0.8712±0.0521	**0.9932±0.0080**
	AUC	0.9244±0.0983	0.8627±0.1268	0.9577±0.0069	0.8951±0.0940	**0.9965±0.0041**
	F-M	0.7045±0.1528	0.4549±0.1158	0.3116±0.0331	0.2418±0.1103	**0.8684±0.0239**
	G-M	0.9151±0.1137	0.8407±0.1573	0.9568±0.0072	0.8914±0.0970	**0.9965±0.0041**
35	ACC	**1±0**	**1±0**	**1±0**	**1±0**	**1±0**
	AUC	**1±0**	**1±0**	**1±0**	**1±0**	**1±0**
	F-M	**1±0**	**1±0**	**1±0**	**1±0**	**1±0**
	G-M	**1±0**	**1±0**	**1±0**	**1±0**	**1±0**
36	ACC	**1±0**	**1±0**	0.9995±0.0008	0.9991±0.0010	**1±0**
	AUC	**1±0**	**1±0**	0.9833±0.0333	0.9666±0.0408	**1±0**
	F-M	**1±0**	**1±0**	0.9818±0.0363	0.9636±0.0445	**1±0**
	G-M	**1±0**	**1±0**	0.9825±0.0348	0.9651±0.0426	**1±0**
37	ACC	0.9990±0.0011	0.9995±0.0009	0.9872±0.0099	**1±0**	0.9995±0.0010
	AUC	0.9797±0.0398	0.9997±0.0004	0.9771±0.0317	**1±0**	0.9833±0.0622
	F-M	0.9595±0.0498	0.9846±0.0307	0.6964±0.1634	**1±0**	0.9818±0.0407
	G-M	0.9786±0.0421	0.9997±0.0004	0.9763±0.0331	**1±0**	0.9826±0.0390
38	ACC	**0.9995±0.0008**	0.9991±0.0011	0.9950±0.0078	0.9991±0.0017	0.9991±0.0012
	AUC	**0.9800±0.0399**	0.9550±0.0556	0.9479±0.0637	0.9600±0.0799	0.9550±0.0622
	F-M	**0.9777±0.0444**	0.9492±0.0630	0.8300±0.2357	0.9500±0.1000	0.9492±0.0705
	G-M	**0.9788±0.0422**	0.9520±0.0593	0.9446±0.0678	0.9549±0.0901	0.9521±0.0664
Performance	ACC	6/38	3/38	3/38	7/38	**31/38**
	AUC	5/38	3/38	4/38	4/38	**34/38**
	F-M	6/38	3/38	3/38	6/38	**32/38**
	G-M	5/38	3/38	4/38	4/38	**34/38**

As shown in Table 6, the proposed algorithm obtained the best performance on 34 datasets for AUC and G-M metrics and on more than 30 datasets for ACC and F-M metrics. This indicates that the proposed algorithm outperforms the four compared algorithms. For example, MNEFD_IE obtains the best performance on Yeast-1-2-8-9-vs-7 with the mean ACC, AUC, F-M, and G-M results of 0.8468, 0.8000, 0.2628, and 0.7954, which are 5.91%, 9.75%, 10.69%, and 10.14% better than the second-best results, respectively.

The average rank number and test results of the above five algorithms are given based on the Friedman aligned rank test and Holm's test in terms of four evaluation metrics. The specific results are shown in Tables 7-8.

Table 7. Average rank numbers of ensemble learning algorithms

Algorithm	ACC	AUC	F-M	G-M
MNEFD_IE	**1.5658**	**1.3816**	**1.5395**	**1.3947**

EASE	2.6053	3.2500	2.6842	3.3684
SPE	3.3158	3.6184	3.4605	3.6316
HUE	4.3816	3.2895	4.1842	3.1053
ECUBoost	3.1316	3.4605	3.1316	3.5000

Table 8. P values from Holm's test

Algorithm	ACC	AUC	F-M	G-M	Hypothesis (0.05)
EASE	2.0387e-04	4.5857e-09	9.3157e-06	1.1536e-10	**Rejected**
SPE	1.3621e-09	6.2702e-12	9.5064e-12	4.9002e-14	**Rejected**
HUE	3.6905e-20	1.1890e-08	1.0609e-17	3.2926e-10	**Rejected**
ECUBoost	8.2446e-08	1.4279e-10	1.5560e-08	7.8126e-12	**Rejected**

As shown in Table 7, the rank numbers of MNEFD_IE in the four evaluation metrics are 1.5658, 1.3816, 1.5395, and 1.3947 in order, which are the lowest. Table 8 shows that the equivalence hypotheses between MNEFD_IE and the compared algorithms are all rejected. Therefore, the proposed algorithm MNEFD_IE outperforms the state-of-the-art imbalanced ensemble algorithms.

To further evaluate the performance of the MNEFD_IE algorithm, the Wilcoxon paired signed-rank test was used to compare the proposed algorithm and the four compared algorithms one by one. The specific results are shown in Table 9.

Table 9. Results of the Wilcoxon pairwise test

Algorithm	Measure	R+	R-	P value	Hypothesis (0.05)
MNEFD_IE vs. EASE	ACC	676	65	1.0708e-05	**Rejected**
	AUC	681	22	8.1248e-07	**Rejected**
	F-M	698	43	2.4761e-06	**Rejected**
	G-M	697	44	5.2082e-06	**Rejected**
MNEFD_IE vs. SPE	ACC	679	24	1.4692e-06	**Rejected**
	AUC	683	20	6.8159e-07	**Rejected**
	F-M	715	26	8.1248e-07	**Rejected**
	G-M	664	39	4.0111e-06	**Rejected**
MNEFD_IE vs. HUE	ACC	697.5	5.5	2.9491e-07	**Rejected**
	AUC	713	28	1.2457e-06	**Rejected**
	F-M	698.5	4.5	2.7019e-07	**Rejected**
	G-M	667.5	35.5	3.5642e-06	**Rejected**
MNEFD_IE vs. ECUBoost	ACC	638.5	64.5	1.5890e-05	**Rejected**
	AUC	685.5	17.5	3.8848e-07	**Rejected**
	F-M	686.5	54.5	4.4861e-06	**Rejected**
	G-M	697.5	43.5	2.6341e-06	**Rejected**

As shown in Table 9, all equivalence hypotheses are rejected, which means that the proposed algorithm outperforms the four compared algorithms. Meanwhile, R+ in the table indicates that the rank sum of MNEFD_IE outperforms the compared algorithm based on 38 datasets, and R- indicates that the rank sum of the compared algorithm outperforms MNEFD_IE. Table 9 shows that R+ is much larger than R-, so MNEFD_IE is significantly better than the state-of-the-art algorithms.

3. Time complexity analysis

The computational complexity of MNEFD_IE consists of the following four components. (1) The Q sample subsets are divided based on the random undersampling method. (2) The initialization of P, U, and V in the MNEFD algorithm is performed by the MNESR and FCM algorithms. (3) Iterative updating of P, U, and V is conducted by the MNEFD algorithm. (4) 2D sparse fusion is performed based on the prediction results.

The computational complexity of the first part is related to the number of sample subsets Q. The second part of initializing P by MNESR involves manifold distance calculation and eigendecomposition, so the complexity is $O\left(N_{min}^3\right)$. The complexity of FCM algorithm to initialize U and V, the complexity is $O\left(N_{min}C^2dt\right)$, where N_{min} is the number of minority class samples, C is the number of clustering centers, d is the sample dimension, and t is the number of iterations in the FCM algorithm. In the third part, the complexities of updating P, U, and V are $O\left(N_{min}^2\right)$, $O\left(N_{min}Cd\right)$, and $O\left(C^2d\right)$, respectively. The computational complexity of the fourth part of the 2D-SFM is related to the number of sample subsets Q and the number of test samples N_t, which can be expressed as $O\left(QN_t\right)$. Assuming that the number of iterations is T, the total computational complexity of the proposed MNEFD_IE algorithm can be expressed as $Q+Q\cdot\left(O\left(N_{min}^3\right)+O\left(N_{min}C^2dt\right)+T\cdot\left(O\left(N_{min}^2\right)+O\left(N_{min}Cd\right)+O\left(C^2d\right)\right)\right)+O\left(QN_t\right)$. It is worth mentioning that in the case of relatively high imbalance ratio, N_{min} is much smaller than the number of total samples, so the increased time cost is not significant and relatively close compared to the classical imbalanced ensemble methods. The specific comparision results of the running time between the proposed MNEFD_ID and the state-of-the-art algorithms are shown in Table 10.

Table 10. The time cost comparison between EASE, SPE, HUE, ECUBoost and MNEFD_IE

ID	EASE (s)	SPE (s)	HUE (s)	ECUBoost (s)	MNEFD_IE (s)
1	0.3383	0.1446	0.2756	1.1255	6.3436
2	0.1966	0.1465	0.1316	1.4987	14.6192
3	0.2413	0.1994	0.1915	1.7194	37.8634
4	0.0929	0.0578	0.0548	1.0686	1.0621
5	0.3690	0.2565	0.6038	2.6864	58.8042
6	0.1409	0.1226	0.1431	1.1678	3.6503
7	0.2542	0.2293	0.4158	2.0981	28.6764
8	0.3655	0.2473	0.5224	1.9837	58.4714
9	0.0977	0.0987	0.0937	1.2348	2.3798
10	0.2536	0.1705	0.2929	1.7264	25.4692
11	0.1176	0.0847	0.1505	1.2563	3.9906
12	0.1189	0.0817	0.1612	1.2865	2.1714
13	0.1017	0.0767	0.1409	1.1774	1.6414
14	0.2227	0.1457	0.3785	2.0747	9.6333

15	0.1027	0.0907	0.1715	1.1882	1.5926
16	0.1317	0.0917	0.1635	1.4541	2.0436
17	0.1236	0.1216	0.1795	1.2366	2.4931
18	0.1207	0.0768	0.1935	1.1289	1.2314
19	0.1605	0.0738	0.2493	1.2199	1.1017
20	0.1238	0.0867	0.2652	1.1741	1.6201
21	0.0897	0.0817	0.2344	1.0877	0.9547
22	0.1498	0.0787	0.2433	1.1359	0.9520
23	0.2054	0.0957	0.3241	1.3310	2.4676
24	0.1011	0.0588	0.2632	1.0033	0.9593
25	0.0887	0.0877	0.3630	1.1617	0.7127
26	0.1253	0.0897	0.5096	1.3894	1.0945
27	0.1667	0.1370	0.6711	2.0650	2.4580
28	0.2253	0.1220	0.8973	1.8235	5.9541
29	0.1635	0.1028	0.5877	1.5818	1.6469
30	0.2962	0.1119	0.5597	1.7273	1.8731
31	0.1428	0.1167	0.5789	2.2304	1.5674
32	0.1326	0.0907	1.1943	1.3666	1.4893
33	0.1256	0.0887	1.1906	1.5584	1.4865
34	0.1593	0.1008	0.2924	1.6109	0.9908
35	0.2664	0.1207	1.2852	2.8180	2.5935
36	0.1534	0.1052	1.1983	2.4106	2.1295
37	0.1466	0.1087	0.3134	2.2223	1.0250
38	0.2048	0.1256	2.1970	2.4046	1.8002

Based on the analysis above, although there is no significant improvement in the computational complexity of the model for the proposed algorithm, the results in Table 6 show that the proposed algorithm has the best classification performance compared to the state-of-the-art algorithms. Therefore, in summary, the proposed algorithm is still highly competitive.

4. Conclusion

Most current imbalanced ensemble algorithms use resampling to preprocess data to obtain balanced subsets for subsequent modeling. However, these algorithms still use original single sample as sample unit for modeling, so they fail to consider the structural information among samples. This limitation leads to low separability, high sensitivity to noise, high overlap among subsets, and so on. Studies show that the structural information between similar samples can solve the above limitation. Therefore, it is necessary to explore how to effectively mine the intersample structural information.

To solve the above problems, we propose a manifold neighboring envelope sample projection reconstruction-based imbalanced ensemble algorithm with consistent fuzzy clustering (MNEFD_IE). The algorithm constructs two types of envelope samples by mining structural information among samples and build the classification model based on the envelope samples rather than the original samples.

Seven classical imbalanced ensemble algorithms, four advanced ensemble learning algorithms and 38 datasets are selected for comparison and verification of the proposed MNEFD_IE. As shown in Table 4, the proposed algorithm MNEFD_IE achieves the best perforamnce compared to the classical

imbalanced ensemble algorithms on more than 30 datasets. Table 6 shows that the proposed algorithm MNEFD_IE obtains the best performance compared to the advanced ensemble learning algoritms on 34 datasets for AUC and G-M metrics and on more than 30 datasets for ACC and F-M metrics. Therefor, it can be determined that the proposed algorithm MNEFD_IE significantly outperforms the classical imbalanced ensemble algorithms and the state-of-the-art algorithms.

In summary, the proposed algorithm achieves satisfactory results, and the following conclusions can be drawn: 1) MNESR can effectively mine the local similarity between the samples and their manifold nearest neighbors and reconstruct it into NES. 2) Consistent fuzzy clustering (CFCMD) can effectively mine the global similarity between samples and map this structural information to the clustering centers, which are high-quality NCES. 3) The proposed algorithm can not only effectively improve the classification accuracy and the diversity of base classifiers but is also generally applicable to high-IR datasets. In addition, the proposed algorithm significantly outperforms the classical and state-of-the-art imbalanced ensemble algorithms.

Although the proposed algorithm is effective and the effectiveness of the envelope samples is verified, further research and improvement are still needed. Multiple-layer clustering to obtain multiple layers of envelope samples can be considered for further verification and improvement. In addition, it is necessary to explore other kinds of clustering algorithms except FCM for further verification and improvement.